Journal of Visualized Experiments

Surface properties of synthesized nanoporous carbon and silica matrices

--Manuscript Draft--

Article Type:	Invited Methods Article - JoVE Produced Video
Manuscript Number:	JoVE58395R4
Full Title:	Surface properties of synthesized nanoporous carbon and silica matrices
Keywords:	nanoporous carbons; Cassie-Baxter model; wettability; modified Washburn equation; microscopic wetting parameter; nitrogen adsorption/desorption isotherms; potentiometric titration; acidity
Corresponding Author:	Malgorzata Sliwinska-Bartkowiak A.Mickiewicz UniversityPoznan Poznan, wielkopolskie POLAND
Corresponding Author's Institution:	A.Mickiewicz UniversityPoznan
Corresponding Author E-Mail:	msb@amu.edu.pl
Order of Authors:	Angelina Sterczyńska
	Małgorzata Zienkiewicz-Strzałka
	Anna Deryło-Marczewska
	Malgorzata Sliwinska-Bartkowiak
Additional Information:	
Question	**Response**
Please indicate whether this article will be Standard Access or Open Access.	Standard Access (US$2,400)
Please indicate the **city, state/province, and country** where this article will be **filmed**. Please do not use abbreviations.	Adam Mickiewicz University, Umultowska 85, 61-614 Poznan, Poland

TITLE:

Surface Properties of Synthesized Nanoporous Carbon and Silica Matrices

AUTHORS & AFFILIATIONS:

Angelina Sterczyńska[1], Małgorzata Zienkiewicz-Strzałka[3], Anna Deryło-Marczewska[3], Małgorzata Śliwińska-Bartkowiak[1,2]

[1]Faculty of Physics, Adam Mickiewicz University, Poznań, Poland
[2]The NanoBioMedical Centre, Poznań, Poland
[3]Department of Physicochemistry of Solid Surface, Faculty of Chemistry, Maria Curie-Skłodowska University, Lublin, Poland

Corresponding Author:

Małgorzata Śliwińska-Bartkowiak (msb@amu.edu.pl)

Email Addresses of the Co-authors:

Angelina Sterczyńska (aster@amu.edu.pl)
Małgorzata Zienkiewicz-Strzałka (malgorzata.zienkiewicz@poczta.umcs.lublin.pl)
Anna Deryło-Marczewska (annad@hektor.umcs.lublin.pl)

KEYWORDS:

Nanoporous carbons, Cassie-Baxter model, wettability, modified Washburn equation, microscopic wetting parameter, nitrogen adsorption/desorption isotherms, potentiometric titration, acidity

SUMMARY:

Here we report the synthesis and characterization of ordered nanoporous carbon (with a 4.6 nm pore size) and SBA-15 (with a 5.3 nm pore size). The work describes the surface and textural properties of nanoporous molecular sieves, their wettability, and the melting behavior of D_2O confined in the materials.

ABSTRACT:

In this work, we report the synthesis and characterization of ordered nanoporous carbon material (also called ordered mesoporous carbon material [OMC]) with a 4.6 nm pore size, and ordered silica porous matrix, SBA-15, with a 5.3 nm pore size. This work describes the surface properties of nanoporous molecular sieves, their wettability, and the melting behavior of D_2O confined in the differently ordered porous materials with similar pore sizes. For this purpose, OMC and SBA-15 with highly ordered nanoporous structures are synthesized *via* impregnation of the silica matrix by applying a carbon precursor and by the sol-gel method, respectively. The porous structure of investigated systems is characterized by an N_2 adsorption-desorption analysis at 77 K. To determine the electrochemical character of the surface of synthesized materials, potentiometric titration measurements are conducted; the obtained results for OMC shows a significant pH_{pzc} shift toward the higher values of pH, relative to SBA-15. This suggests that investigated OMC has surface properties related to oxygen-based functional groups. To describe

the surface properties of the materials, the contact angles of liquids penetrating the studied porous beds are also determined. The capillary rise method has confirmed the increased wettability of the silica walls relative to the carbon walls and an influence of the pore roughness on the fluid/wall interactions, which is much more pronounced for silica than for carbon mesopores. We have also studied the melting behavior of D_2O confined in OMC and SBA-15 by applying the dielectric method. The results show that the depression of the melting temperature of D_2O in the pores of OMC is about 15 K higher relative to the depression of the melting temperature in SBA-15 pores with a comparable 5 nm size. This is caused by the influence of adsorbate/adsorbent interactions of the studied matrices.

INTRODUCTION:

In 1992, ordered nanoporous silica materials were obtained for the first time, using an organic template; since then, a large number of publications related to different aspects of these structures, synthetic methods, the investigation of their properties, their modifications, and different applications have appeared in the literature[1-3]. The interest in SBA-15 nanoporous silica matrix[4] is due to their unique quality: a high surface area, wide pores with a uniform pore size distribution, and good chemical and mechanical properties. Nanoporous silica materials with cylindrical pores, such as SBA-15[5], are often used as a porous matrix for catalysts as they are efficient catalysts in organic reactions[6-7]. The material can be synthesized with a wide range of methods that can influence their characteristics[8-10]. Therefore, it is crucial to optimize these methods for potential applications in many fields: electrochemical devices, nanotechnology, biology and medicine, drug delivery systems, or in adhesion and tribology. In the present study, two different types of nanoporous structures are presented, namely silica and carbon porous matrices. To compare their properties, the SBA-15 matrix is synthesized using the sol-gel method, and the ordered nanoporous carbon material is prepared by the impregnation of the resulting silica matrix with a carbon precursor.

Porous carbon materials are important in many appliances due to their high surface area and their unique and well-defined physicochemical properties[6,11-12]. Typical preparation results in materials with randomly distributed porosity and a disordered structure; there is also a limited possibility for the change of the general pore parameters, and thus, structures with relatively broad pore size distributions are obtained[13]. This possibility is broadened for nanoporous carbon materials with high surface areas and ordered systems of nanopores. More predicted geometry and more control of the physicochemical processes inside the pore space are important in many applications: as catalysts, separation media systems, advanced electronic materials, and nanoreactors in many scientific fields[14-15].

To obtain the porous carbon replicas, the ordered silicates can act as a solid matrix to which carbon precursors are directly introduced. The method can be divided into several stages: the selection of ordered silica material; the deposition of a carbon precursor in a silica matrix; carbonization; then, the removal of the silica matrix. Many different types of carbonaceous materials can be obtained by this method, but not all nonporous materials have an ordered structure. An important element of the process is the selection of a suitable matrix whose nanopores must form a stable, three-dimensional structure[16].

In this work, the influence of the type of pore walls on the surface properties of synthesized nanoporous matrices is investigated. The surface properties of OMC material are reflected by the surface properties of silica analog (SBA-15) of OMC. The textural and structural properties of both types of materials (OMC and SBA-15) are characterized by low-temperature N_2 adsorption/desorption measurements (at 77 K), transmission electron microscopy (TEM), and energy dispersive X-ray analysis (EDX).

Low-temperature gas adsorption/desorption measurement is one of the most important techniques during the characterization of porous materials. Nitrogen gas is used as an adsorbate due to its high purity and the possibility to create a strong interaction with solid adsorbents. Important advantages of this technique are the user-friendly commercial equipment and relatively easy data-processing procedures. The determination of nitrogen adsorption/desorption isotherms is based on the accumulation of the adsorbate molecules on the surface of solid adsorbent at 77 K in a wide range of pressure (P/P_0). The Barrett, Joyner, and Halenda (BJH) procedure for calculating the pore size distribution from experimental adsorption or desorption isotherms is applied. The most important assumptions of the BJH method include a planar surface and an even distribution of the adsorbate on the investigated surface. However, this theory is based on the Kelvin equation and it remains the most widely used manner for calculating the pore size distribution in the mesoporous range.

To evaluate the electrochemical character of the samples, a potentiometric titration method is applied. The surface chemistry of the material depends on the surface charge related to the presence of heteroatoms or functional groups on the surface. The surface properties are also investigated by contact angle analysis. The wettability inside the pores provides information about the adsorbate-adsorbent interactions. The influence of the wall roughness on the melting temperature of the water confined in both samples is studied with the dielectric relaxation spectroscopy (DRS) technique. Measurements of the dielectric constant allow the investigation of melting phenomena as the polarizability of the liquid and solid phases are different from each other. A change in the slope of the temperature dependence of the capacitance shows that melting occurs in the system.

PROTOCOL:

1. Preparation of the OMC Materials

1.1. Synthesis of a silica matrix as OMC precursor

1.1.1. Prepare 360 mL of 1.6 M HCl by adding 50 mL of HCl (36% - 38%) in a 500 mL round-bottom flask and, then, adding 310 mL of ultrapure water (resistivity of 18.2 MΩ·cm).

1.1.2. To that, add 10 g of PE 10500 polymer (6.500 g/mol).

1.1.3. Place the flask in an ultrasonic bath. Heat the solution to 35 °C and stir it until the solid polymer is completely dissolved, making a homogeneous mixture.

1.1.4. Add 10 g of 1,3,5-trimethylbenzene to the flask and stir the content (at a stirring rate of 220 rpm) by maintaining it at 35 °C in the water bath.

1.1.5. After stirring for 30 min, add 34 g of tetraethyl orthosilicate (TEOS) to the flask. Add the TEOS slowly and dropwise with constant stirring. Ensure that it takes 10 min to add 34 g of TEOS.

1.1.6. Stir the solution mixture again for 20 h at the same temperature (35 °C).

1.1.7. Transfer the contents of the flask into a polytetrafluoroethylene cartridge and place it in an autoclave. Leave the solution for 24 h at 90 °C.

1.1.8. Filter the resulting precipitate, using a Büchner funnel, and wash it with distilled water, using at least 1 L.

1.1.9. Dry the obtained solid at room temperature and apply a thermal treatment to the sample at 500 °C, using a muffle furnace in an air atmosphere for 6 h.

1.2. Impregnation of the resulting silica matrix, using a carbon precursor

1.2.1. Prepare impregnation solutions (IS1 and IS2) with appropriate proportions of water, 3 M sulfuric acid (VI), and sugar (glucose), where glucose plays the role of carbon precursor and sulfuric acid acts as catalyst.

CAUTION: **Sulfuric acid is very toxic**, it causes severe skin burns and eye damage.

1.2.1.1. Prepare IS1. For each gram of silica, mix 5 g of water, 0.14 g of 3 M sulfuric acid (VI), and 1.25 g of sugar.

1.2.1.2. Prepare IS2. For each gram of silica, mix 5 g of water, 0.08 g of 3 M sulfuric acid (VI), and 0.75 g of sugar.

1.2.2. Place the silica material (1 g) and the prepared solution IS1 of the carbon precursor and the catalyst in a 500 mL flask. Heat the mixture in a vacuum dryer at 100 °C for 6 h.

NOTE: In this step, use only IS1. IS2 should be applied in the next step.

1.2.3. Add the IS2 to the mixture in the vacuum dryer (to the solution with the partially carbonized carbon precursor). Heat the mixture again in the vacuum dryer at 160 °C for 12 h.

1.3. Tempering/carbonization

1.3.1. Transfer the obtained composite to a mortar for the fragmentation of the larger particles and a homogenization of the material.

1.3.2. Place the obtained product into the flow furnace and heat it to 700 °C (at a heating rate of 2.5 °C/min) and heat for 6 h at this temperature. Heat the material in a nitrogen atmosphere.

1.3.3. Allow the solution to cool before opening the furnace.

1.4. Removal of the silica matrix by etching

1.4.1. Prepare 100 mL of etching solution (ES). Mix 50 mL of 95% ethyl alcohol and 50 mL of water. Add 7 g of potassium hydroxide and stir until it is dissolved.

1.4.2. Place all obtained carbonized material (at least 1 g) in a 250 mL round-bottom flask and add 100 mL of ES.

1.4.3. Supply the system with a reflux condenser and magnetic stirrer and heat to a boil while stirring constantly. Boil the mixture for 1 h.

1.4.4. Transfer the obtained material to the Büchner funnel, wash it with at least 4 L of distilled water, and dry it.

2. Preparation of the Silica SBA-15 Matrix

2.1. Synthesize a silica matrix.

2.1.1. Prepare 150 mL of 1.6 M HCl.

2.1.2. Dissolve 4 g of PE 6400 polymer ($EO_{13}PO_{70}EO_{13}$) in 150 mL of acid solution in a round-bottom flask.

2.1.3. Place the flask in an ultrasonic bath. Heat the solution to 40 °C and stir it so that the polymer can dissolve (at least for 30 min).

2.1.4. Slowly add 8.5 g of TEOS to the flask, dropwise, with constant stirring. Stir the solution mixture for 24 h at the same temperature (40 °C).

2.1.5. Transfer the contents of the flask to a polytetrafluoroethylene cartridge. Leave the solution for 24 h in a 120 °C oven.

2.1.6. Filter the resulting precipitate, using a Büchner funnel, and wash it with distilled water (at least 1 L).

2.1.7. Dry the obtained solid at room temperature and calcine for 6 h at 600 ° C, using a muffle furnace in an air atmosphere.

3. Methods of Characterization

3.1. Low-temperature nitrogen adsorption/desorption measurements

3.1.1. Use an automatic sorption analyzer to obtain N_2 adsorption/desorption isotherms at 77 K.

3.1.2. Use an appropriate glass tube for nitrogen sorption measurements. Before adding the porous sample to the glass tube, clean the tube in an ultrasonic washer and rinse it first with distilled water and, next, with anhydrous ethanol.

3.1.3. Heat the glass tube at 150 °C for 3 h and fill the tube with compressed nitrogen. Weigh the empty glass tube under the nitrogen conditions before the measurement to minimize the weight error.

3.1.4. Place the sample in the glass tube and weigh the total mass (the mass of the sample with the glass tube).

3.1.5. Prior to the measurements, degas the sample. Place the glass tube with the sample in the degassing port of the sorption analyzer. Apply the following process conditions: a pressure of at least 0.01 mmHg, a temperature of 423 K, and a duration of 24 h. In the degassing port, connect the sample to the vacuum and heat it to the set temperature (423 K). After degassing, fill the sample with nitrogen and transfer it to the analysis port.

3.2. Transmission electron microscopy

3.2.1. Use the TEM microscope with the 120 kV (for SBA-15) and 200 kV (for the OMC material) accelerating voltages to collect the good quality TEM images.

3.2.2. For preparing a monodisperse film of the sample, disperse the sample (1 mg) in ethanol (1 mL). Perform the dispersion procedure in a microcentrifuge tube by placing it in an ultrasonic bath for 3 min.

3.2.3. Place two drops of the dispersion on a TEM copper grid using a micropipette. Transfer the TEM grid to the TEM microscope and start the TEM imaging.

3.3. Energy dispersive X-ray spectroscopy

3.3.1. Use a scanning electron microscope equipped with an X-ray detector to acquire an energy dispersive X-ray spectrum of the samples.

3.3.2. Apply an acceleration voltage of 15 kV to harvest the spectrum. Select the silicon as the optimization element for SBA-15 and the carbon for the OMC sample.

3.4. Potentiometric titration measurement

3.4.1. Use an automatic burette to perform the potentiometric titration experiment. Add the titrant in small and controlled portions (according to the titration software and procedure). Provide the smallest increment, at least 1 µL, by an automatic dosing intrument.

3.4.2. Disperse 0.1 g of the sample in 30 mL of an electrolyte solution (water solution of 0.1 M NaCl). Use the magnetic stirrer and isothermal conditions (293 ± 0.1 K) during the dispersion procedure.

3.4.3. Add 1 - 2 mL of titrant (0.1 M NaOH solution) to the suspension.

NOTE: Perform the addition in small aliquots (each to be about 0.05 mL). The automatic burette ensures the stability of the titrant amount added during this process. After each step, specify the pH of the suspension. The procedure should provide at least a dozen experimental points in the pH range from 1 to 14.

3.4.4. Calculate the surface density of the charge Q_s, using the following formula.

$$Q_s = \frac{F\Delta n}{S_{BET}} \quad (1)$$

Here,
Δn = the change in H^+/OH^- balance reduced per mass of sample;
S_{BET} = the Brunauer-Emmett-Teller (BET) surface area of the porous solid state;
F = the Faraday number.

3.5. Capillary rise method for wettability measurements

3.5.1. To determine the contact angle inside the pores of the studied samples, use the capillary rise method.

NOTE: This method is based on the measurement of the mass rise of the liquid, which is penetrating the porous bed, as the function of the time. The main assumption of this method is based on the fact that penetrating liquid is advancing into the porous column and that this column consists of intergranular capillaries with a certain average radius. Thus, every relation derived for single capillary is valid for the layer of the porous powder. In a single vertical capillary, the wetting liquid floats against the gravitational forces as a result of the difference of pressure between the liquid and the vapor in the pores (capillary pressure). In this meaning, the penetration of the liquid into the porous bed allows the determination of the dynamic advancing contact angle inside the pores.

3.5.2. Apply the modified Washburn's equation[17-18], expressed as follows.

$$m^2 = \frac{C\rho^2\gamma_l \cos\theta}{\eta} t \quad (2)$$

Here,
m = the mass of the measured liquid;
C = the geometric parameter dependent on the distribution, shape, and size of the pores;
ρ = the density;
γ_l = the surface tension;
η = the viscosity of the penetrating liquid;
θ = the contact angle;
t = time.

3.5.3. Using equation (2), estimate the values of the advancing contact angles inside the studied pores.

3.5.4. Prepare the force tensiometer. For powders, use a glass tube with a diameter of 3 mm and a ceramic sinter; for liquid, use a vessel with a diameter of 22 mm and a maximum volume of 10 mL.

3.5.5. Measure 0.017 g of the sample.

3.5.6. Start the computer program connected to the tensiometer. Put a vessel with the liquid on a motor-driven stage and suspend the glass tube with the sample on an electronic balance.

3.5.7. Start the motor and start approaching the liquid in the vessel with the sample at a low constant rate of 10 mm/min; set the immersion depth of the sample tube into the liquid equal to 1 mm.

3.5.8. From this moment, the dependence $m^2 = f(t)$ registers in the computer program.

3.5.9. Stop the experiment when the dependence $m^2 = f(t)$ starts to show the characteristic plateau.

3.5.10. Check for accuracy by repeating this procedure 3x - 5x.

3.6. Dielectric relaxation spectroscopy

3.6.1. To describe the melting behavior of confined water inside the studied porous matrices, perform the temperature measurements of electric capacitance C of the sample present in a parallel plate capacitor made of stainless steel[19-21]. To measure the capacitance C as the function

of the temperature and the frequency of the applied cyclic electric field, use an impedance analyzer.

NOTE: The complex electric permittivity is defined as $\varepsilon^* = \varepsilon` + i\varepsilon``$, where $\varepsilon` = C/C_0$ is the real, and $\varepsilon`` = tg\delta \cdot \varepsilon`$ is an imaginary part of the permittivity, where C_0 is the capacitance of the empty capacitor and $tg\delta$ are the dielectric losses.

3.6.2. Put the measured sample into the plate capacitor.

3.6.3. Select a frequency range from 100 Hz to 1 MHz and a temperature from 140 K to 305 K. Control the rate of temperature change with the temperature controller; set the temperature rate as equal to 0.8 K/min during the cooling and 0.6 K/min during the heating process.

REPRESENTATIVE RESULTS:

To characterize the porous structure of the investigated samples of OMC and SBA-15, the N_2 adsorption-desorption isotherms were recorded at 77 K. The experimental N_2 gas adsorption-desorption isotherms characterizing the investigated systems, as well as the pore size distributions (PSD) obtained from the adsorption and desorption data, are presented in **Figure 1A-D**. The position of the inflection points on the sorption isotherms (**Figure 1A, C**) indicates the pressure at which the process of mesopore filling starts. This information is needed for the calculation of the mean pore size and the PSD (**Figure 1B, D**), according to the Kelvin equation.

Figure 2A-C presents the TEM images of the OMC. **Figure 2D, E** presents the TEM images of the SBA-15 sample. The obtained TEM micrographs were used for evaluating the quality of the synthesized materials and confirming the two-dimensional hexagonal structure. An interpretation of the TEM images allows an estimation of the pore sizes and a comparison of the values with the data obtained from sorption measurements (**Figure 1**).

Figure 3 shows the surface charge density distribution for carbon and silica material. The properties of surfaces and interfaces of supports and solid matrices have a crucial impact on the characteristics of investigated materials and on the physicochemical processes and phenomena on their surface or in their vicinity. An experimental investigation of the surface properties, such as surface charge densities, seems to be appropriate and valuable for investigating how surface properties (presence and types of functional groups) influence the investigated chemical and physical phenomena. In particular, the surface characteristics related to the surface chemistry of the carbon materials depend on the surface charge defined by heteroatoms (such as oxygen or nitrogen) and influence the wettability, adsorptive properties, electrochemical and catalytic features, and finally, acid–base and hydrophilic–hydrophobic behavior. An analysis of the point-of-zero charge position on the pH scale provides information about the system's acidity; the lower the pH_{pzc} value, the more acidic the sample is.

Figure 4A, B shows typical TEM-energy dispersive X-ray spectroscopy (EDS) spectra for the OMC sample illustrating the interaction of the incident electron beam with the sample, which generates the X-rays with energies characteristic of an atomic number of elements. TEM-EDS is

a powerful tool for the determination of the chemical composition. **Figure 4C** shows the EDS results for SBA-15 material. The value of the energy of the characteristic radiation coming from the sample allows an identification of the elements contained in the studied sample, while the intensity (the height of the peaks in the spectrum) enables a qualitative analysis of its contents (**Figure 4C**).

Figure 5 depicts the results of the measurements of contact angles inside the nanopores of OMC (**Figure 5A**) and SBA-15 (**Figure 5B**), referenced to the wettabilities on smooth highly oriented pyrolytic graphite (HOPG) and glass substrates, respectively. An ideally smooth silica surface glass and HOPG graphite as a smooth graphite surface were used. The measured contact angles are shown as a function of the microscopic wetting parameter α_w for both the smooth planar silica, the graphite surface, and the rough nanoporous materials. Values of α_w for the liquids on these silica and graphite substrates (**Figure 5A, B**) can be found based on the following equation.

$$\alpha_w = \frac{\rho_w \sigma_{fw}^2 \Delta \varepsilon_{fw}}{\varepsilon_{ff}} \quad (3)$$

Here,
ε_{fw}, ε_{ff} = the energy depths of the Lennard-Jones potential;
σ_{fw} = the collision length of the Lennard-Jones potential;
ρ_w = the number of solid atoms per unit volume;
Δ = the distance between the separating layers in the substrate.

These values are taken from previously published literature[22-24]. The measurement of wettability allows the characterization of the adsorbate/adsorbent interactions. Together with the potentiometric titration and EDX analysis, the measurement of wettability provides a full description of the surface properties of a given sample. The lower the contact angle, the higher the wettability, which means that the interaction of the penetrating liquid molecule with the studied surface is stronger (**Figure 5A, B**).

Figure 6 shows the roughness fractions f calculated from the Cassie-Baxter model[25] *vs.* the microscopic wetting parameter for the nanoporous carbon (OMC; **Figure 6A**) and the silica (SBA-15; **Figure 6B**) matrix. We assume that the wetting on the rough surfaces occurs according to the Cassie-Baxter mechanism (*i.e.,* the droplet of the liquid does not penetrate the cavities but is on the top of the irregularities [as shown in the insets of **Figure 5A, B**]). In this model, the contact angle on the rough surface θ_p is described as:

$$\cos\theta_p = f(1 + \cos\theta) - 1 \quad (4)$$

Here,
θ = the contact angle value on a smooth nonporous substrate (glass);
f = is the fraction of the porous surface which is in direct contact with the liquid interface.

It is worth evaluating the roughness fractions *f* (equation 4) which acts as a correction factor for interpreting contact angle measurements for the liquid molecules with the sample surface in the pores.

Figure 7 presents the dielectric spectroscopy results for deuterated water confined in the studied samples of OMC (**Figure 7A**) and SBA-15 (**Figure 7B**). These illustrate the temperature dependences of electric capacity *C* for both samples (**Figure 7A, B**). In the solid state of the polar substance, their orientational polarization vanishes, and the dielectric constant ε is equal to n^2, where *n* is the refractive index of the substance. The sharp increase visible in the *C*-T curves indicates the melting phase transitions occurring in the system. The temperature of the anomalous increase of the *C*-T function allows the determination of the melting point of both the bulk liquid and the melting point in the pores of the studied sample.

FIGURE AND TABLE LEGENDS:

Figure 1: Experimental N_2 adsorption/desorption isotherm plot at 77 K and porosity distributions by the Barrett, Joyner, and Halenda method (BJH)[7, 26-27]. For (**A** and **B**) nanoporous carbon material and (**C** and **D**) silica SBA-15 material. The nitrogen isotherms show characteristic hysteresis loops, providing an information about the shape and pore size distributions of the studied pores.

Figure 2: TEM images illustrating the ordered nanoporous channels structure. (**A** - **C**) TEM images of the nanoporous carbon along the (001) direction at various magnifications. (**D** - **E**) The structure of SBA-15.

Figure 3: Potentiometric titration results for OMC and SBA-15 (pH dependence of the surface charge density). The surface charge density dependence of pH shows the differences in the electrochemical character of both materials; the pzc point provides information about the number of acid sites on the sample surface.

Figure 4: Examples of TEM- EDS spectra and EDS analysis. (**A** and **B**) EDS spectra for the OMC sample, recorded from two different areas marked on the TEM image. (**C**) EDS spectra and quantitative analysis result of the SBA-15 sample. Quantitative results of an EDS analysis give information about the presence of elements in the functional groups responsible for the surface reactivity; this is a technique complementary to the potentiometric titration.

Figure 5: Contact angles *vs.* the microscopic wetting parameter measured inside the porous matrices. (**A**) The nanoporous carbon (OMC) and (**B**) silica (SBA-15) matrix, referenced to as the contact angles *vs.* the microscopic wetting parameter function on smooth HOPG and glass substrates, respectively. The wettability inside the pores refers to the wettability on flat surfaces and provides some information about the influence of the pore roughness on adsorbate/adsorbent interactions.

Figure 6: The roughness fractions *f* calculated from the Cassie-Baxter model *vs.* the microscopic wetting parameter. For (**A**) the nanoporous carbon (OMC) and (**B**) silica (SBA-15) matrix. An application of the Cassie-Baxter model of wettability allows the interpretation of contact angles on rough porous substrates. The *f* fractions calculated from this model describe the percentage of contributions of the porous wall which are in direct contact with the liquid surface.

Figure 7: Temperature dependences of electric capacitance of D_2O water confined inside the OMC and SBA-15 porous matrix. The (**A**) OMC and the (**B**) SBA-15 porous matrix. The interpretation of the *C*-T function allows the identification of the temperature of the phase transition of D_2O in pores and in the bulk occurring in the studied system. An increase in *C*-T function lead to the increase in melting point for both bulk water and confined water inside the pores. The value of the melting point's shift in pores relative to the bulk is dependent on the host/guest molecular interactions.

Table 1: The values of textural parameters describing a porous structure of ordered nanoporous carbon and SBA-15 silica calculated from N_2 sorption isotherms. [a]BET surface area calculated using experimental points at the relative pressure of (P/P_0) 0.035 - 0.31, where P and P_0 are denoted as the equilibrium and saturation pressure of nitrogen. [b]Surface area and pore volume of micropores calculated by the t-plot method with a fitted statistical thickness in the range from 3.56 to 4.86 Å. [c]Total pore volume calculated by 0,0015468 x the amount of nitrogen adsorbed at P/P_0 = 0.99. [d]Hydraulic pore diameters calculated from the BET surface areas and pore volumes according to the equation: $D_h = 4V/S$. [e]The pore diameter estimated from the PSD maximum of the nonlocal density functional theory (NLDFT). NLDFT calculations were performed using a nonnegative regularization of 0.001 and the cylindrical geometry of pores as a model of carbon porosity. [f]The pore diameter estimated from the BJH method (the same results for adsorption and desorption data). *The lack of values of pore diameters of SBA-15 estimated from the NLDFT method.

DISCUSSION:

The critical steps during the preparation of the ordered mesoporous carbon material include the preparation of the ordered mesoporous silica materials as the template with well-defined structural properties that affect the properties of the final materials and a tempering/carbonization step under a nitrogen atmosphere. The modification of the typical method of preparation of the mesoporous ordered silicates with cylindrical pores[28] concerns the application of an untypical structure-directing agent that is PE10500 polymer, for the improvement of the structural properties of the material. The three-dimensional, interconnected, and stable porous structure of the template is necessary for the preparation of the mesoporous carbon materials. Moreover, a key disadvantage of the preparation is the essential requirement of the sample treatment for the template removal. The properties of chemicals used in this step can affect the carbon surface and its functionality. According to the presented strategy, the preparation of the negative replication of OMC is based on the ordered mesoporous solid template. The pore size control and symmetric ordering are simply determined using the silica template and are not associated with the interaction between the carbon precursor and the template. The potential of OMC for various electrochemical systems has been

indicated in the literature[29-30]. The impregnation mechanism presented in this work is responsible for the facile process to precisely replicate the negative structure of the silica template. The nature of the hard template procedure ensures that the pyrolysis phenomena cause less damage to the regular and ordered structure. Moreover, this method allows an easier graphitization of the OMC materials formed within the solid template.

The experimental N_2 adsorption/desorption isotherm (**Figure 1A, C**) was used to obtain preliminary information about the type and size of porosity. The nanoporous character of the material was clearly confirmed. A small increase in the quantity of nitrogen adsorbed in the initial stage of the process (in the range of relative pressure below 0.03) and its significant increase in the further range of relative pressure (especially in the range of mesopores) indicates the existence of a significant number of mesopores and the lack, or a very small number, of micropores. The adsorption-desorption isotherms obtained for this material are typical of type-IV (IUPAC classification[31]), which is a correct reflection of the carbon mesoporous channel system with a sharp capillary condensation stage at intermediate relative pressure (0.45 - 0.9 P/P_0). The position of the capillary condensation step corresponds to the primary size of mesopores (about 4 - 5 nm). The investigated carbon sample exhibits also a high specific surface area (757 $m^2 \cdot g^{-1}$) and a significant pore volume (0.87 $cm^3 \cdot g^{-1}$).

The critical steps during nitrogen adsorption/desorption measurements are the very precise mass sample determination step and the sufficiently degas step. The measurement procedure was performed according to the appropriate guidelines. Despite the fact that the determination of the surface area and the pore size distribution is based on the physisorption measurements, the interpretation of the experimental isotherms is not always direct.

During the computation of the mesopores' size distribution, by application of the modified Kelvin equation (which is the basis of the theory), it is necessary to accept the assumption of the rigid pores of well-defined shape. Moreover, the range of validity of the Kelvin equation and the interpretation of hysteresis loops on the isotherms remain unresolved problems. The possibility of facilitation is related to the application of empirical methods of isotherm analysis (*e.g.*, the α_s-method[29-34]). However, this manner requires the use of adsorption data obtained with nonporous reference materials.

Figure 1B, D presents the mesopores' size distributions of studied samples (PSD). The assumption of the BJH theory permitted the determination of the mesopores' size distribution. The PSD curve presented in **Figure 1B** suggests that the carbon sample contained mesopores of the sizes of 3.5 - 4 nm, whereas SBA-15 possessed pores with a diameter of about 5 nm (see **Figure 1D**). Interestingly, for the OMC sample, the maxima of the pore size distribution curves calculated from adsorption and desorption data are very similar. Such as accurate agreement between the results, in view of different mechanisms of adsorption and desorption phenomena, evidence a very ordered and uniform nature of the material. The textural properties determined from experimental isotherms are summarized in **Table 1**.

The properties of the pore network structure based on the physical adsorption/desorption analyses are fundamental to the characterization of nanopowders and nanomaterials. Nitrogen adsorption/desorption methods can be regarded as the first stage in the characterization of microporous and mesoporous solids. The method is, in general, applicable to samples of all classes of porous bodies or materials and allows an estimation of the porous structures on the basis of the shapes of isotherms and hysteresis loops directly from the experimental measurement. The nitrogen adsorption/desorption next to the other methods of porous structure determination (liquid intrusion[35] and light, X-ray, and neutron scattering[36-37] and microscopy[32]) is the most important and useful technique due to the wide applicability and mutual comparability of the results.

Nitrogen is a standard adsorptive gas molecule for pore characterization by gas adsorption method. It is possible to use other types of molecules (carbon dioxide, krypton, argon) for obtaining new information about the sample and for the characterization of microporous materials.

The TEM micrographs of investigated OMC and SBA-15 samples are presented in **Figure 2**. They confirmed a highly ordered system of mesopores, comprising of parallel and very similar porous channels and a carbon rod-shaped structure with the pore size ~11 nm (**Figure 2A-C**). TEM micrographs of OMC confirmed a hexagonal symmetry of the pores as a result of the inverse replica of the initial nanoporous silica precursor and a pore diameter between the rods of 4.0 nm. The SBA-15 sample shows the two-dimensional ordered hexagonal structure of the mesopores; the well-ordered structure of SBA-15 is observed in both projections, along with the nanoporous channels and perpendicular to them (**Figure 2D, E**). These observations are in good agreement with the values obtained from the experimental nitrogen sorption data (see **Table 1**). Transmission electron microscopy is able to provide images at a higher resolution than light microscopy due to the smaller de Broglie wavelength of the electrons. This enables us to capture the details thousands of times smaller than a resolvable object seen in a light microscopy. In this method, the image comes from the interaction of the electrons with the sample when the beam is transmitted throughout the specimen. Therefore, one of the limitations of the method is that the specimen should be an ultrathin film of less than 100 nm thick or a suspension applied on a grid. TEM can be improved on by a scanning transmission electron microscope (STEM). It should be possible by an addition of a system combined with suitable detectors, which will raster the beam across the sample to form the image.

The pH of the point-of-zero charge of OMC (*i.e.*, the pH value below which the total surface of the carbon particles is positively charged) was found to be above pH = 10 (**Figure 3**). For comparison, the pH of the point-of-zero charge of the SBA-15 material is equal to about 4.5. Potentiometric titration results of SBA-15 material show a shift of pH_{pzc} toward lower pH values, evidencing of the existence of some acid centers on the SBA-15 surface. The negatively charged sites increase the Van der Waals interactions between the adsorbent/adsorbate molecules in the SBA-15 matrix, improving the adsorptive properties of the silica matrix.

The critical steps during potentiometric titration measurement include the very precise addition of the titrant to the suspension and continuity of stirring. The potentiometric titration procedure was fully automated to ensure the most reliable results. Another important and unique step was the application of special software for controlling experimental conditions and calculations. The limitation of this method is the calibration step of the pH electrode and the need to ensure a stable atmosphere (for example, nitrogen) and temperature. Potentiometric titration can be categorized as an acid/base titration procedure. This technique requires measurements of the voltage change upon titrant addition steps. It provides an adaptable, affordable, and highly accurate technique to achieve high purity, which is essential in many fields, particularly in pharmaceuticals and functional material studies. In fact, there are a number of types of potentiometric titrations. There are, for instance, acid-base, redox, precipitation, and complexometric techniques. As potentiometric titrations can be realized automatically, it ensures greater capacity for sample characterization.

The pzc is determined as the intersection of the electrolyte titration curve and the titration curve recorded for carbon material, as well as the intersection of the surface charge density curve with the axis. The result suggests that investigated, ordered nanoporous carbon material has basic properties related to the presence of oxygen functional groups (-OH terminal groups of ketonic, pyronic ring, chromenic, and π-electron systems)[38-41]. The basic properties of the carbon surface can be a result of a thermal treatment that causes progressive destruction and removal of acidic oxygen functional groups (for example, carboxyls, lactones, and phenols) and, thus, enriches the carbon surface in basic functional groups[42]. The presence of these basic sites is a consequence of the simultaneous decrease in the number of acidic sites and a reduction of oxygen content associated directly with the acidity. The content of oxygen was verified by the TEM-EDS.

TEM-EDS spectra images of the OMC surface from two different areas of the sample are displayed in **Figure 4A, B**. Oxygen and silicon atoms from the OMC surface were detected despite the predominant amount of carbon. The atomic and weight percentage of the elements, presented as insets and obtained from different areas of the samples, are similar and indicate about 98% is composed of carbon and only slightly more than 1% of the composition is attributable to oxygen. EDS microanalysis may suggest that the basic character of the OMC surface is associated with very low number of oxygen-containing functional groups, which typically has acidic functionality. Moreover, the basic functional groups can be responsible for the growing of hydrophilicity of the carbon materials. An EDS spectrum of silica matrix confirms the main contribution of oxygen and silicon abundance in the SBA-15 (**Figure 4C**). EDX is one of the techniques that determine the atomic composition of the specimen. It does not give chemical information (*e.g.*, oxidation state, chemical bonds), like an XPS method. For quantitative analysis, EDX is not suitable for light elements (*e.g.*, like oxygen) since it can only detect the presence of oxygen but cannot quantitate it. This method works only on the surface of thin layers (of a few microns or less) and is quite sensitive to the contamination in the specimen.

In **Figure 5 A, B** the results of contact angle measurements for several liquids on silica and carbon substrates are presented; we can see that the systems reveal a wide range of wettabilities. Two of the applied substrates are smooth and planar, namely the silica and carbon surfaces, while the

others show roughness and contain mesopores. The measured contact angles are presented *vs.* the microscopic wetting parameter, α_w. This parameter is the ratio between the liquid-pore wall intermolecular interactions to the interactions of two liquid molecules[22-24]. Therefore, it measures the wetting properties at the nano- and macroscales. The α_w parameter is shown to be a monotonic function of the contact angle. According to the measurements, the values of contact angles for the surfaces with roughness are higher than those for the smooth planar surfaces, irrespective of the type of studied liquids, including nonwetting and well-wetting liquids.

These results suggest the Cassie-Baxter mechanism of wettability on nanorough surfaces of porous walls. Moreover, the contact angles measured for several liquids inside silica and carbon nanopores indicate better wettability of the silica walls than the carbon walls, and the influence of pore roughness on the fluid/wall interactions is more pronounced for silica than for carbon nanopores. The capillary rise method is used to determine the contact angles and wettability of small particles in the powders. For a flat solid substrate, many techniques, such as sessile drop method and Wilhelmy plate method, can be applied to contact angle measurements. The use of capillary rise method assumes the satisfaction of four conditions during the process (*i.e.*, Washburn's equation is derived based on these four assumptions): (1) a constant laminar flow, (2) the absence of an external pressure, (3) negligible gravitational force, and (4) the liquid at the solid-liquid interface does not move. The hydrostatic pressure is much smaller than the capillary pressure; therefore, the capillary pressure causes the liquid to rise upward along the tube. The wettability studies of small particles should always take into account the accuracy and reproducibility of the results.

To measure accurately the contact angle of small particles, the pressure increments and the hydrostatic effects should be taken into account in Washburn's equation to more accurately describe the relationship between the pressure increment and time.

In **Figure 6A, B**, we present the fraction f (describing the part of a porous surface which is in direct contact with the liquid interface), defined as $f = (1 + \cos\theta_p) / (1 + \cos\theta)$. It takes values from the range of 0.73 (H_2O) to 0.92 (OMCTS) for silica matrix and from the range of 0.82 (H_2O) to 0.93 (OMCTS) for carbon matrix. Moreover, the fraction f increases monotonically with the increasing α_w parameter, which confirms the Cassie-Baxter model of wetting on rough substrates.

These results, discussed within the framework of the Cassie-Baxter model, show that for nanosurfaces, the influence of microroughness significantly affects changes in the fluid-wall interactions.

To investigate the influence of the character of the porous surfaces on the confinement effects of D_2O in SBA-15 and OMC matrices with a comparable pore size of 5 nm, the dielectric method was used. The results of the electric capacity of water placed in OMC and SBA-15 upon heating, as presented in **Figure 7A** and **Figure 7B**, respectively, indicate that the temperature dependence of capacitance C shows a sharp increase at T = 260 K, corresponding to the melting of adsorbed D_2O inside the pores of SBA-15, and at T = 246.1 K, which refers to the melting of water adsorbed inside the pores of OMC. For both systems, we observe an increase in the C(T) function at T =

276.5 K, which is referred to the melting point of the bulk deuterated water. The observed signals are related to both the bulk and the confined liquid because the samples are studied as suspension in filled porous matrices with the liquid being in excess. Relative to that of the bulk, the melting temperature of D_2O in SBA-15 pores is depressed by $\Delta T = T_{m,pore} - T_{m,bulk} = -16.5$ K, while for OMC, $\Delta T = -30.4$ K.

These results come from various structures of the pore wall. The melting temperature in the pores $T_{m,pore}$ is dependent on two variables, namely the pore size H and the wettability parameter α_w. For smaller α_w values ($\alpha_w < 1$), the depression of $T_{m,pore}$ is expected. If the pore width H is the same, then the change in the α_w value of the system affects the change in $T_{m,pore}$. The results of the wettability in pores show that the α_w value in both systems studied decreases due to the roughness effects relative to those of the smooth surface. The work of immersed wettability in pores $W_e = \gamma_l \cos\theta_p$ is much less for D_2O in OMC (W_e = 4,2432 [mN/m]) than in SBA-15 (W_e = 20,968 [mN/m]), which leads to a high depression of the melting point in this system, relative to that for D_2O in the SBA-15 system.

The obtained results indicate an improvement in the adhesion effects on the porous silica wall, relative to those on the carbon wall. This method has some limitations when applied to the studied samples. One of them comes from the fact that the record of the $C(T)$ function contains the signal from both the bulk liquid and the liquid confined in the pores. Therefore, the signal from the confined nonpolar liquid is weak, and it is difficult to determine the melting temperature. In the future, it is worth combining some additional methods along with it. (*e.g.*, differential scanning calorimetry on a slow heating rate or centrifuging the sample to get concentrated sample without any liquid). Moreover, for the conductive samples, there is a need to use a polytetrafluoroethylene plate. An advantage of dielectric spectroscopy method is the fact that the method is used a lot, in many areas of research, such as glass transitions and time-scale molecular motions, where the time length is in the tens of femtoseconds to nanoseconds. Therefore, it is important to provide frequencies ranging from megahertz to terahertz. In cases such as decomposition of the obtained spectra or the interpretation and quantitative analysis of the results, the technique resembles more common spectroscopies. However, the dielectric method investigates the collective fluctuations of molecules with a permanent dipole moment (polar liquids). For example, infrared spectroscopy provides additional complementary information, although the sensitivity in the direction of collective modes may impede the interpretation of dielectric spectra.

ACKNOWLEDGMENTS:

The authors would like to thank the National Center of Science for providing financial support with grant no. DEC-2013/09/B/ST4/03711 and UMO-2016/22/ST4/00092. The authors are also grateful for the partial support from the Poland Operational Program *Human Capital* PO KL 4.1.1, as well as from the National Centre for Research and Development, under research grant no. PBS1/A9/13/2012. The authors are especially grateful for Prof. L. Hołysz from Interfacial Phenomena Division, Faculty of Chemistry, Maria Curie-Skłodowska University, Lublin, Poland, for her kindness and enabling the measurements of the wettability in the SBA-15 nanopores.

DISCLOSURES:

The authors have nothing to disclose.

REFERENCES:

1. Tao, Y., Kanoh, H., Abrams, L., Kaneko, K. Mesopore-Modified Zeolites: Preparation, Characterization, and Applications. *Chemical Reviews.* **106**, 896-910 (2006).
2. Wan, Y., Zhao, D. On the Controllable Soft-Templating Approach to Mesoporous Silicates. *Chemical Reviews.* **107**, 2821-2860 (2007).
3. Khder, A. E. S., Hassan, H. M. A., El-Shall, M. S. Acid catalyzed organic transformations by heteropolytungstophosphoric acid supported on MCM-41. *Applied Catalysis A.* **411-412**, 77-86 (2012).
4. Zhao, D. D. *et al.* Triblock Copolymer Syntheses of Mesoporous Silica with Periodic 50 to 300 Angstrom Pores. *Science.* **279**, 548-552 (1998).
5. Linssen, T., Cassiers, K., Cool, P., Vansant, E. Mesoporous templated silicates: an overview of their synthesis, catalytic activation and evaluation of the stability. *Advances in Colloid and Interface Science.* **103**, 121-147 (2003).
6. Eftekhari, A., Fan, Z. Ordered mesoporous carbon and its applications for electrochemical energy storage and conversion. *Materials Chemistry Frontiers.* **1**, 1001-1027 (2017).
7. Sing, K. Characterization of porous materials: past, present and future. *Colloids and Surfaces A.* **241**, 3-7 (2004).
8. Huo, Q., Margolese, D. I. Generalized synthesis of periodic surfactant/inorganic composite materials. *Nature.* **368**, 317−321 (1994).
9. Selvaraj, M., Kawi, S., Park, D. W., Ha, C. S. Synthesis and characterization of GaSBA-15: Effect of synthesis parameters and hydrothermal stability. *Microporous and Mesoporous Materials.* **117**, 586-595 (2009).
10. Leonard, A. *et al.* Toward a better control of internal structure and external morphology of mesoporous silicas synthesized using a nonionic surfactant. *Langmuir.* **19**, 5484-5490 (2003).
11. Liang, C., Li, Z., Dai, S. Mesoporous Carbon Materials: Synthesis and Modification. *Angewandte Chemie International Edition.* **47**, 3696-3717 (2008).
12. Babić, B. *et al.* New mesoporous carbon materials synthesized by a templating procedure. *Ceramics International.* **39**(4), 4035-4043 (2013).
13. Allen, S.J., Whitten, L., Mckay, G. The Production and Characterization of Activated Carbons: A Review. *Developments in Chemical Engineering and Mineral Processing.* **6**, 231-261 (1998).
14. Kwak, G. *et al.* Preparation Method of Co_3O_4 Nanoparticles Using Ordered Mesoporous Carbons as a Template and Their Application for Fischer–Tropsch Synthesis. *The Journal of Physical Chemistry C.* ***117*** (4), 1773-1779 (2013).
15. Koo, H.M. *et al.* Effect of the ordered meso–macroporous structure of Co/SiO2 on the enhanced activity of hydrogenation of CO to hydrocarbons. *Catalysis Science and Technology*. **6**, 4221-4231 (2016).
16. Jun, S., Joo, S.H., Ryoo, R., Kruk, M., Jaroniec, M. Synthesis of New, Nanoporous Carbon with Hexagonally Ordered Mesostructure. *Journal of the American Chemical Society.* **122** (43), 10712-10713 (2000).
17. Washburn, E.W. The dynamics of capillary flow. *Physical Review Series 2.* **17**, 273 (1921).

781 18. Śliwińska-Bartkowiak, M., Sterczyńska, A., Long, Y., Gubbins, K.E. Influence of Microroughness
782 on the Wetting Properties of Nano-Porous Silica Matrices. *Molecular Physics.* **112**, 2365-2371
783 (2014).
784 19. Śliwińska-Bartkowiak, M. *et al.* Melting/freezing behavior of a fluid confined in porous glasses
785 and MCM-41: dielectric spectroscopy and molecular simulation. *Journal of Chemical Physics.* **114**,
786 950-962 (2001).
787 20. Coasne, B., Czwartos, J., Śliwińska-Bartkowiak, M., Gubbins, K.E. Freezing of mixtures
788 confined in silica nanopores: experiment and molecular simulation. *Journal of Chemical Physics*
789 **133**, 084701-084709 (2010).
790 21. Chełkowski, A. *Dielectric Physics*. PWN-Elsevier. Warsaw, Poland (1990).
791 22. Radhakrishnan, R., Gubbins, K.E., Śliwińska-Bartkowiak, M. Global phase diagrams for freezing
792 in porous media. *Journal of Chemical Physics*. **116**, 1147-155 (2002).
793 23. Gubbins, K.E., Long, Y., Śliwińska-Bartkowiak, M. Thermodynamics of confined nano-phases.
794 *Journal of Chemical Thermodynamics.* **74**, 169-183 (2014).
795 24. Radhakrishnan, R., Gubbins, K.E., Śliwińska-Bartkowiak, M. Effect of the fluid-wall interaction
796 on freezing of confined fluids: Toward the development of a global phase diagram. *Journal of*
797 *Chemical Physics.* **112**, 11048 (2000).
798 25. Cassie, A.B.D., Baxter, S. Wettability of porous surfaces. *Transactions of the Faraday Society*.
799 **40**, 546 (1944).
800 26. Sing, K. Adsorption methods for the characterization of porous materials. *Advances in Colloid*
801 *and Interface Science.* **76-77**, 3-11 (1998).
802 27. Sing, K. The use of nitrogen adsorption for the characterisation of porous materials. *Colloids*
803 *and Surfaces A.* **187-188**, 3-9 (2001).
804 28. Yu, C., Fan, J., Tian, B., Zhao, D. Morphology Development of Mesoporous Materials: a
805 Colloidal Phase Separation Mechanism. *Chemistry of Materials.* **16** (5), 889-898 (2004).
806 29. Liu, D. *et al.* Enhancement of Electrochemical Hydrogen Insertion in N-Doped Highly Ordered
807 Mesoporous Carbon. *The Journal of Physical Chemistry C.* **118** (5), 2370-2374 (2014).
808 30. Choi, W. C. *et al.* Platinum Nanoclusters Studded in the Microporous Nanowalls of Ordered
809 Mesoporous Carbon. *Advanced Materials.* **17**, 446-451 (2005).
810 31. Rouquerol, F., Rouquerol, J., Sing, K. *Adsorption by Powders and Porous Solids: Principles,*
811 *Methodology and Application.* Academic Press. London, UK (1999).
812 32. Gregg, S.J., Sing, K.S.W. *Adsorption, Surface Area and Porosity*. Academic Press. London, UK
813 (1982).
814 33. Llewellyn, P. L., Rouquerol, F., Rouquerol, J., Sing, K. S. W. Critical appraisal of the use of
815 nitrogen adsorption for the characterization of porous carbons. In *Characterization of Porous*
816 *Solids V.* Edited by Unger, K. K., Kreysa, G., Baselt J. P., Studies in Surface Science and Catalysis
817 128, 421-427, Elsevier. Amsterdam, The Netherlands (2000).
818 34. Sing, K. S. W. The use of gas adsorption for the characterization of porous solids. *Colloids and*
819 *Surfaces.* **38**, 113-124 (1989).
820 35. Rouquerol, J. Recommendations for the characterization of porous solids. *Pure & Applied*
821 *Chemistry.* **66**, 1739-1758 (1994).
822 36. Marega, C. A direct SAXS approach for the determination of specific surface area of clay in
823 polymer-layered silicate nanocomposites. *The Journal of Physical Chemistry B.* **116**, 7596-7602
824 (2012).

37. Tsao, C. S. *et al.* Neutron Scattering Methodology for Absolute Measurement of Room-Temperature Hydrogen Storage Capacity and Evidence for Spillover Effect in a Pt-Doped Activated Carbon. *The Journal of Physical Chemistry Letters.* **1**, 1569-1573 (2010).
38. Mattson, J. S., Mark, H. B. *Activated Carbon: Surface Chemistry and Adsorption from Solution*. Dekker. New York, NY (1971).
39. László, K., Szucs, A. Surface characterization of polyethyleneterephthalate (PET) based activated carbon and the effect of pH on its adsorption capacity from aqueous phenol and 2,3,4-trichlorophenol solutions. *Carbon.* **39**, 1945-1953 (2001).
40. Garten, V.A., Weiss, D.E., Willis, J.B. A new interpretation of the acidic and basic structures in carbons. *Australian Journal of Chemistry.* **10**, 309-328 (1957).
41. Boehm, H. P. Surface oxides on carbon and their analysis: A critical assessment. *Carbon.* **40**, 145-149 (2002).
42. Menendez, J.A., Phillips, J., Xia, B., Radovic, L. R. On the modification and characterization of chemical surface properties of activated carbon: In the search of carbons with stable basic properties. *Langmuir.* **12**, 4404-4410 (1996).

Fig 1

Click here to access/download;Figure;Fig.1-1.pdf

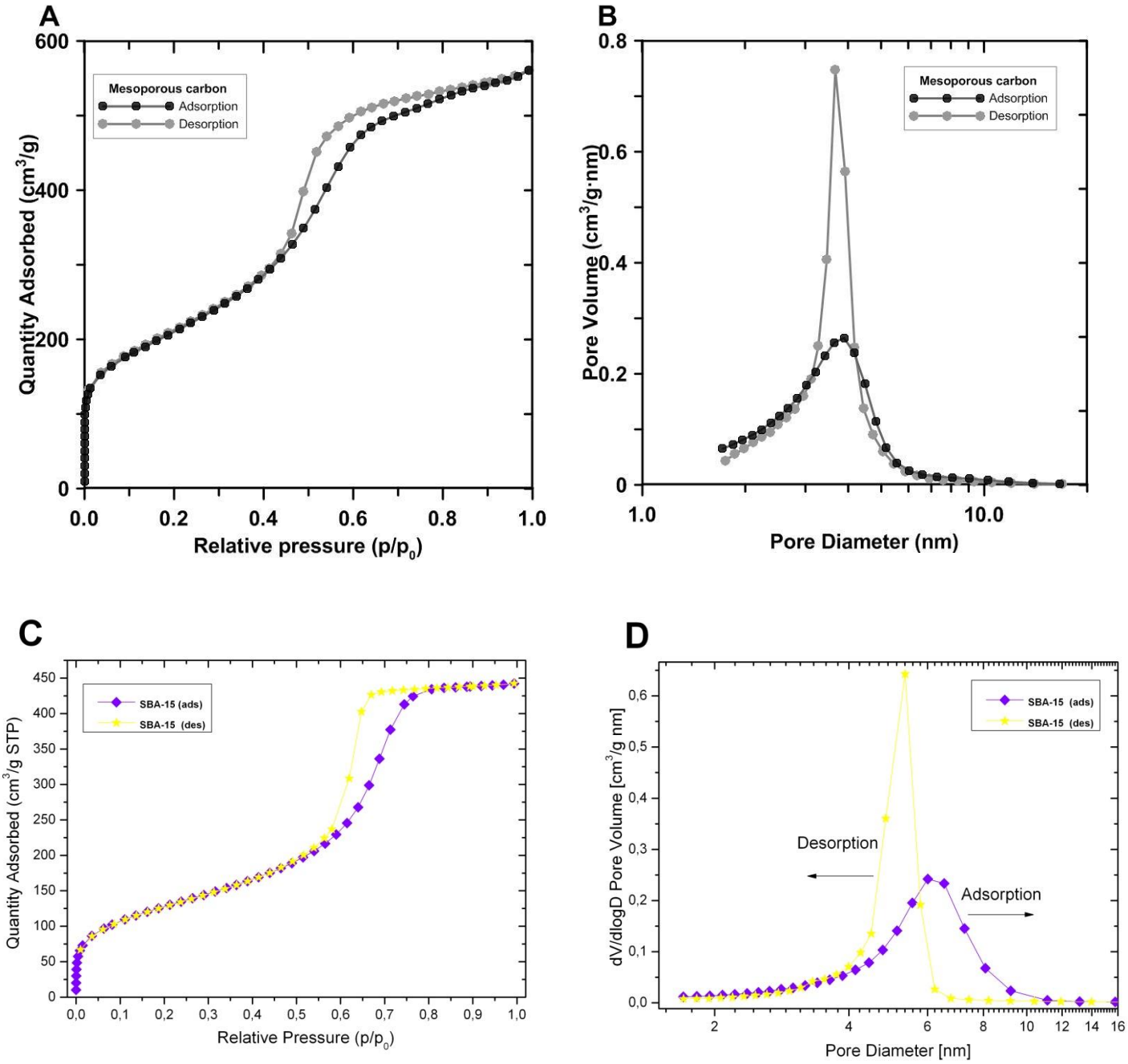

Fig 2

Click here to access/download;Figure;Fig.2.pdf

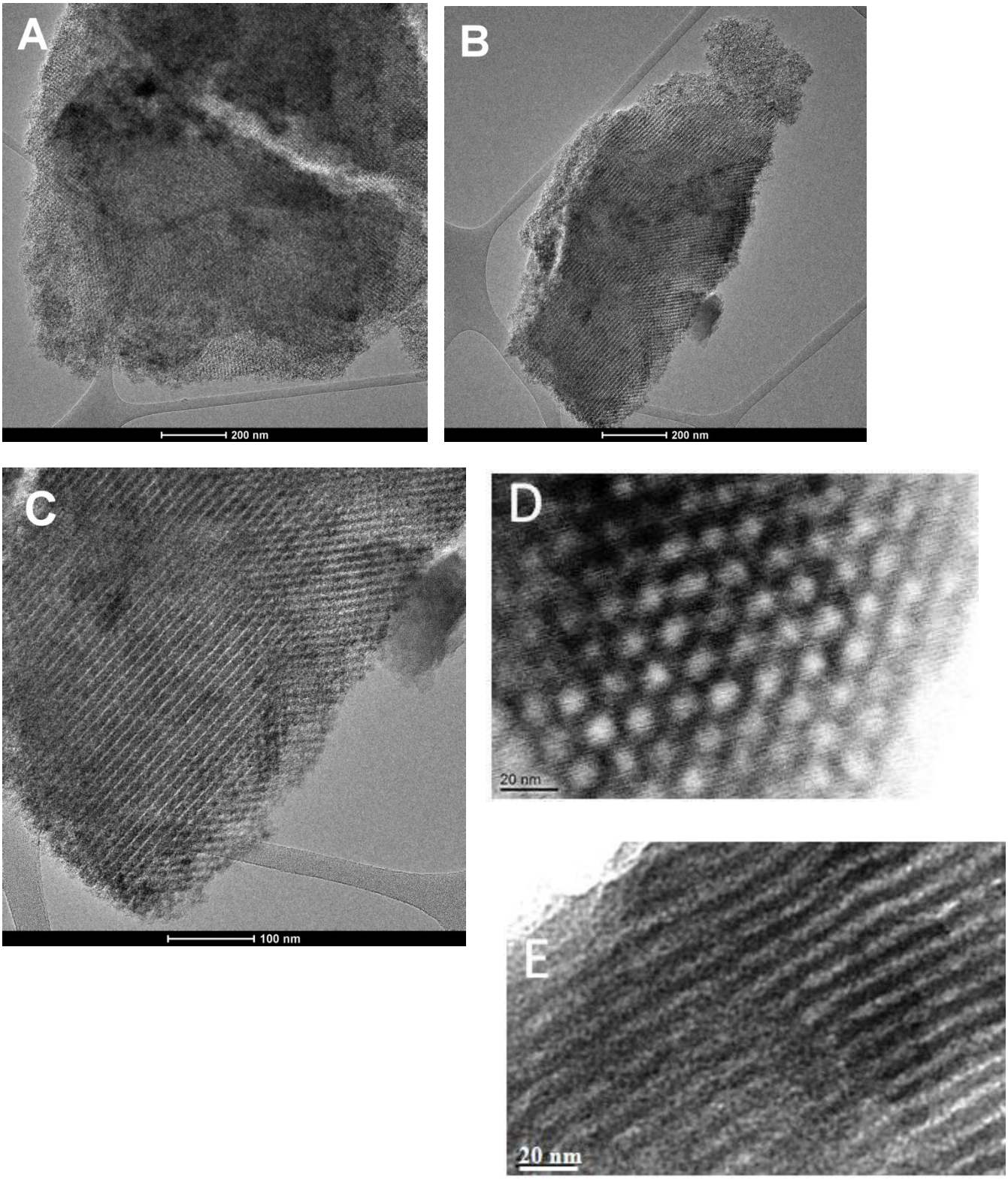

Fig 3

Click here to access/download;Figure;Fig.3-3.jpg

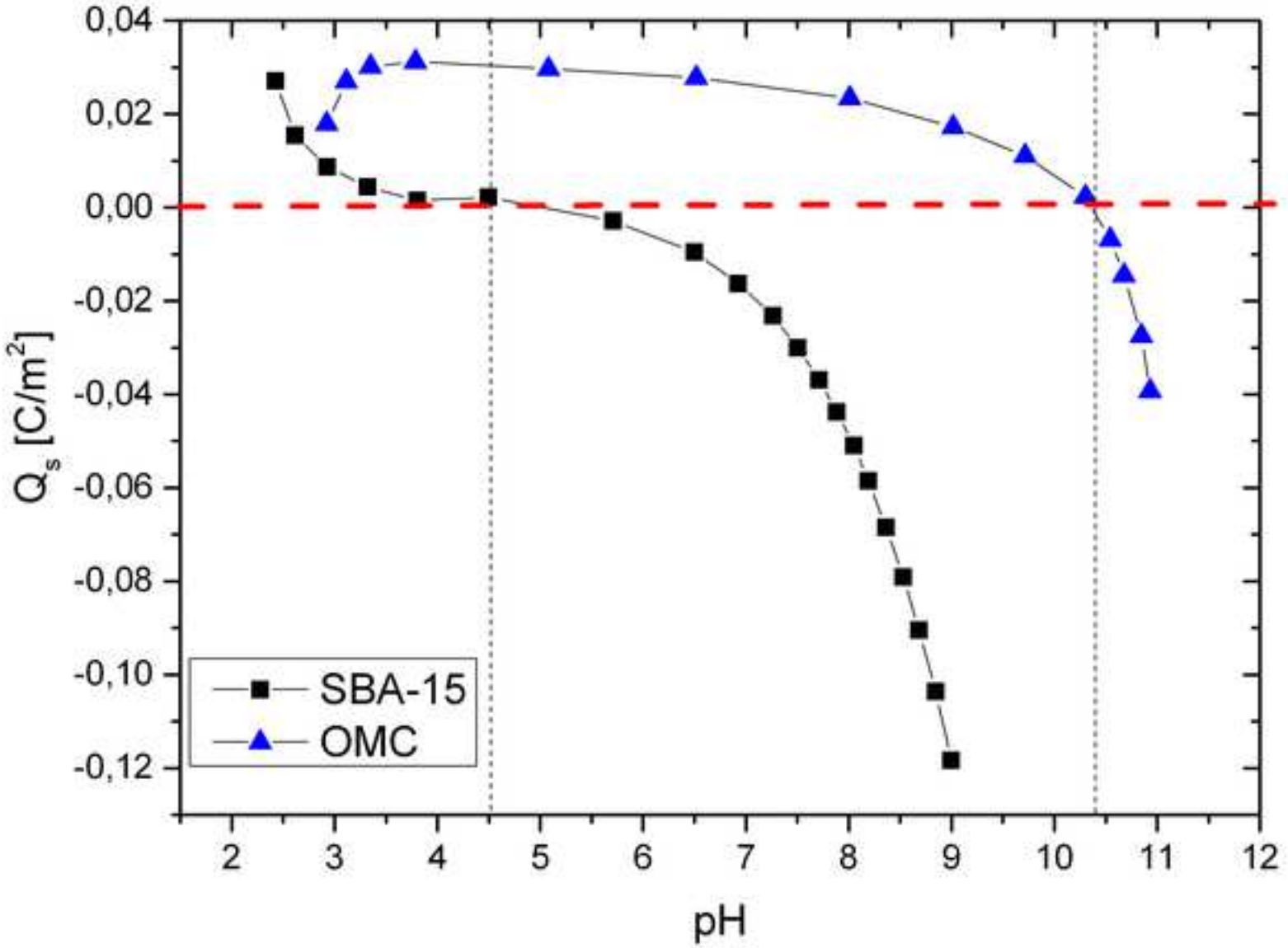

Fig 4

Click here to access/download;Figure;Fig.4.pdf

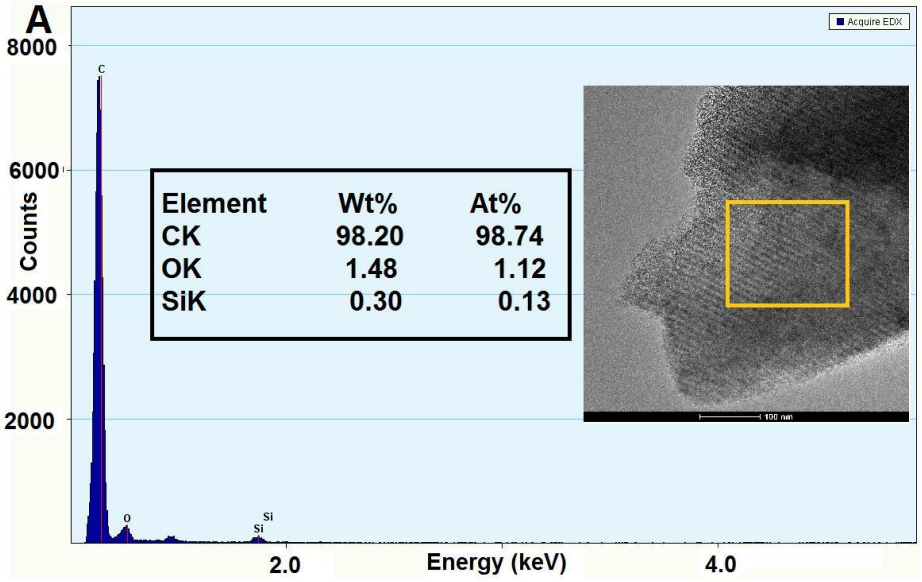

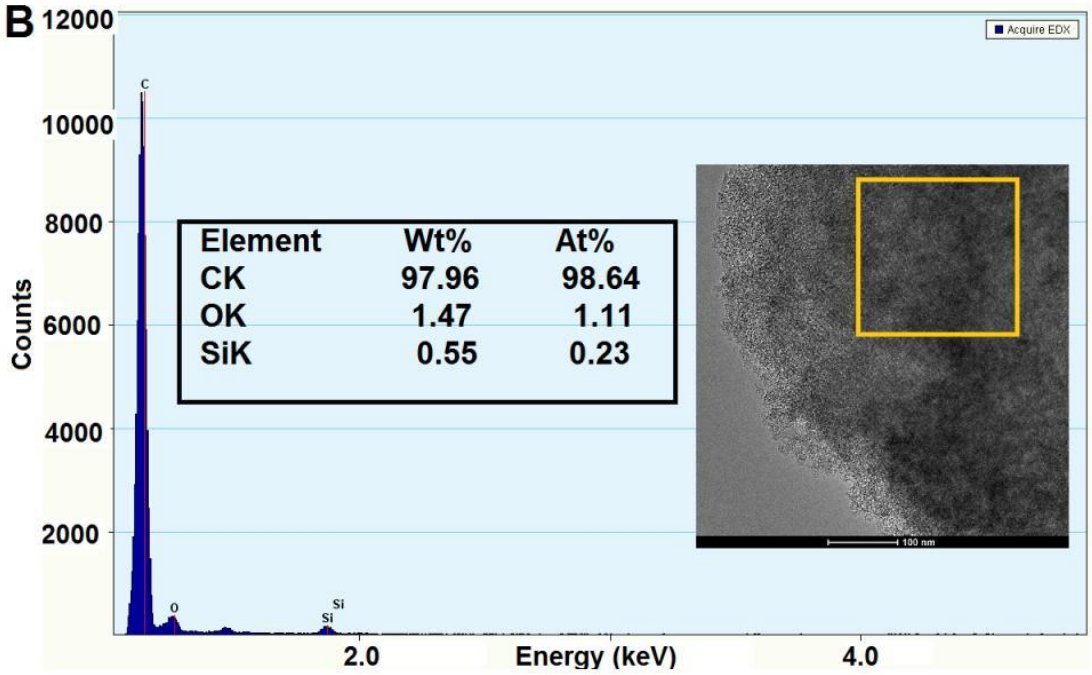

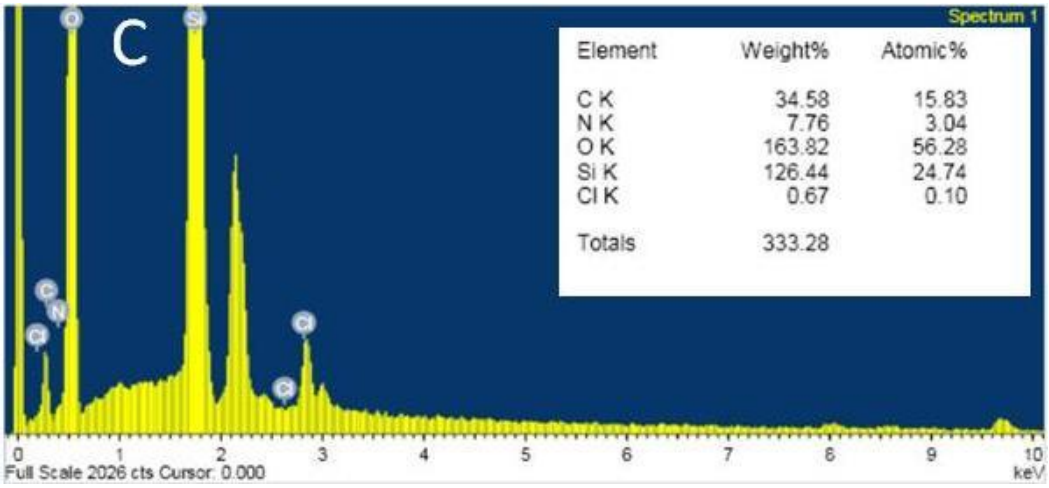

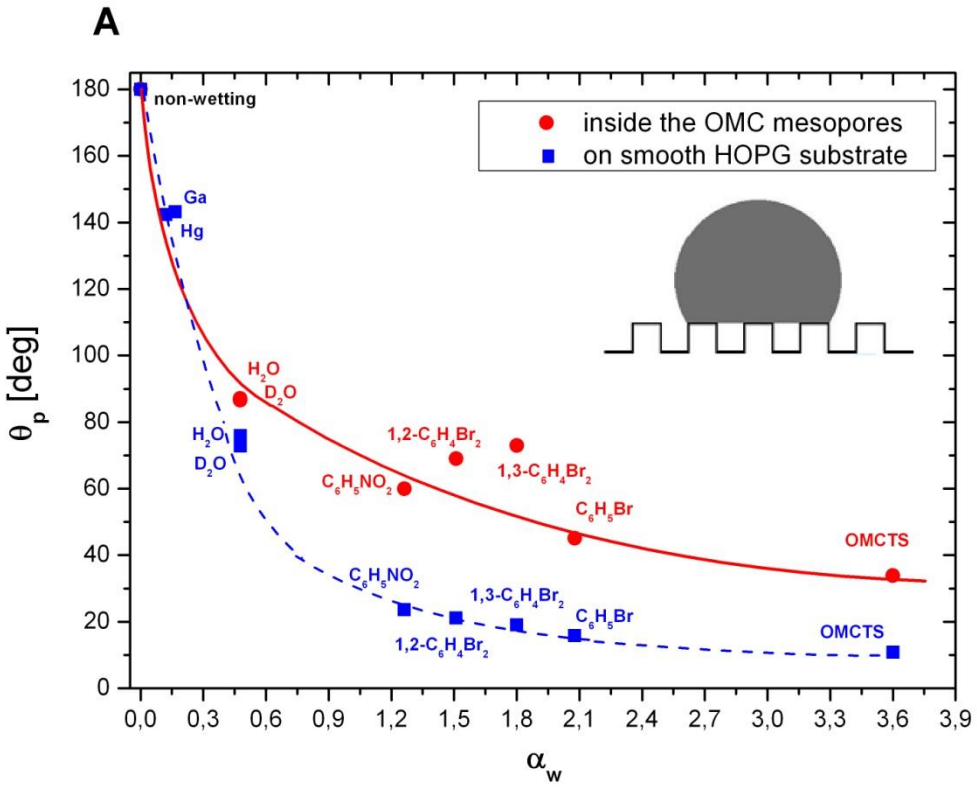

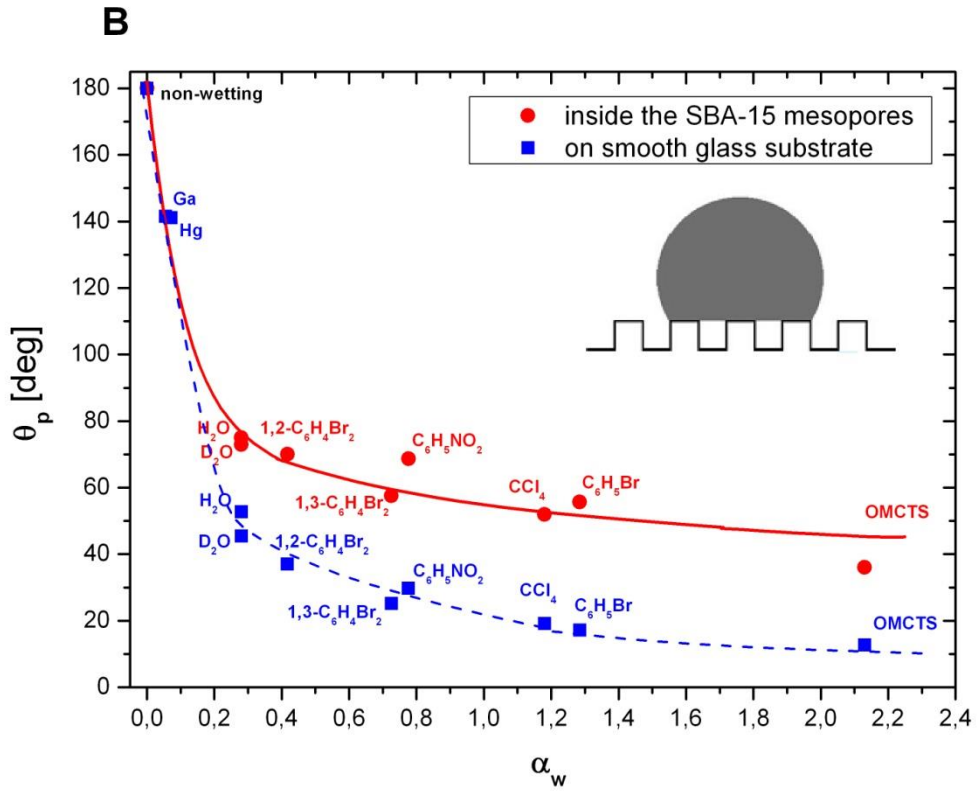

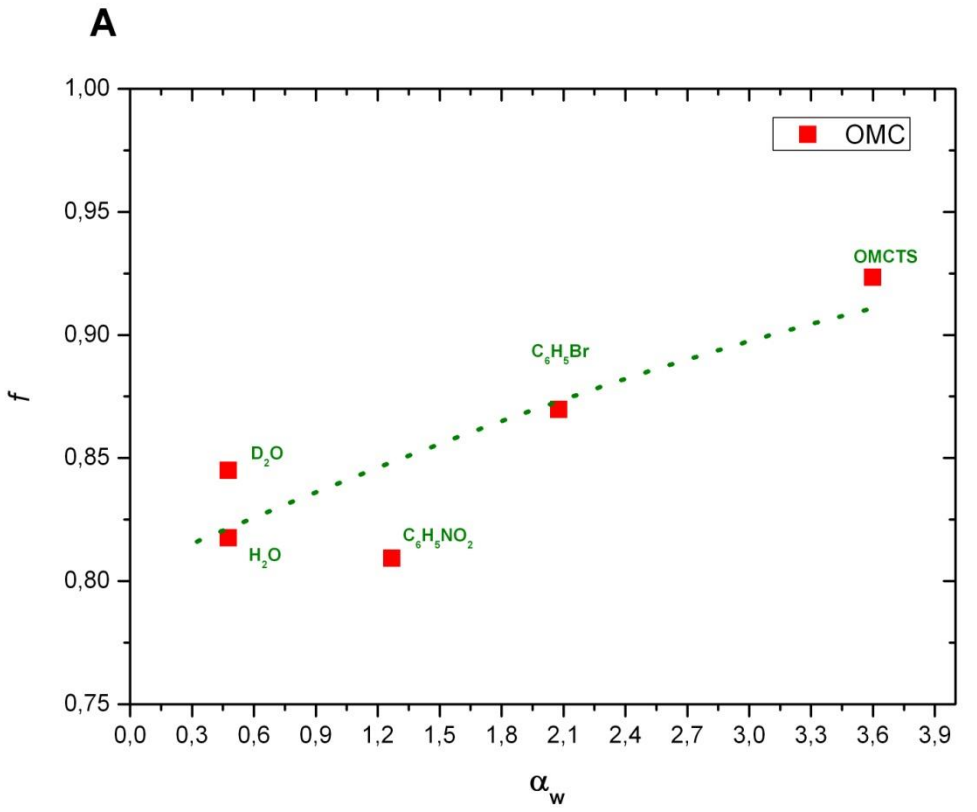

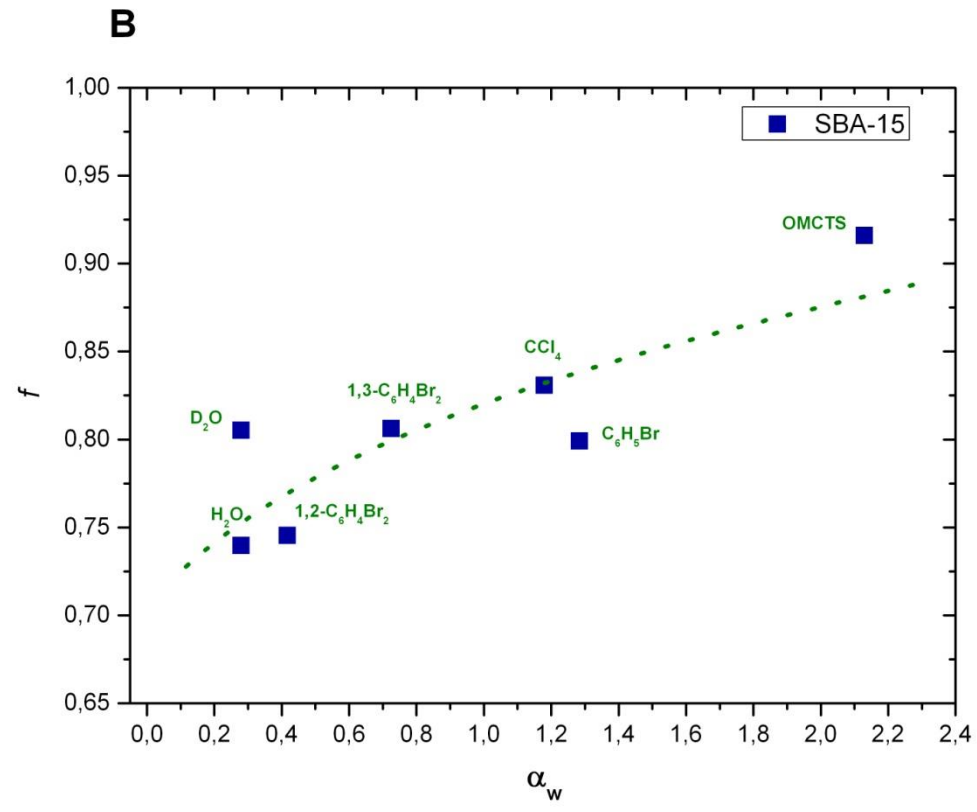

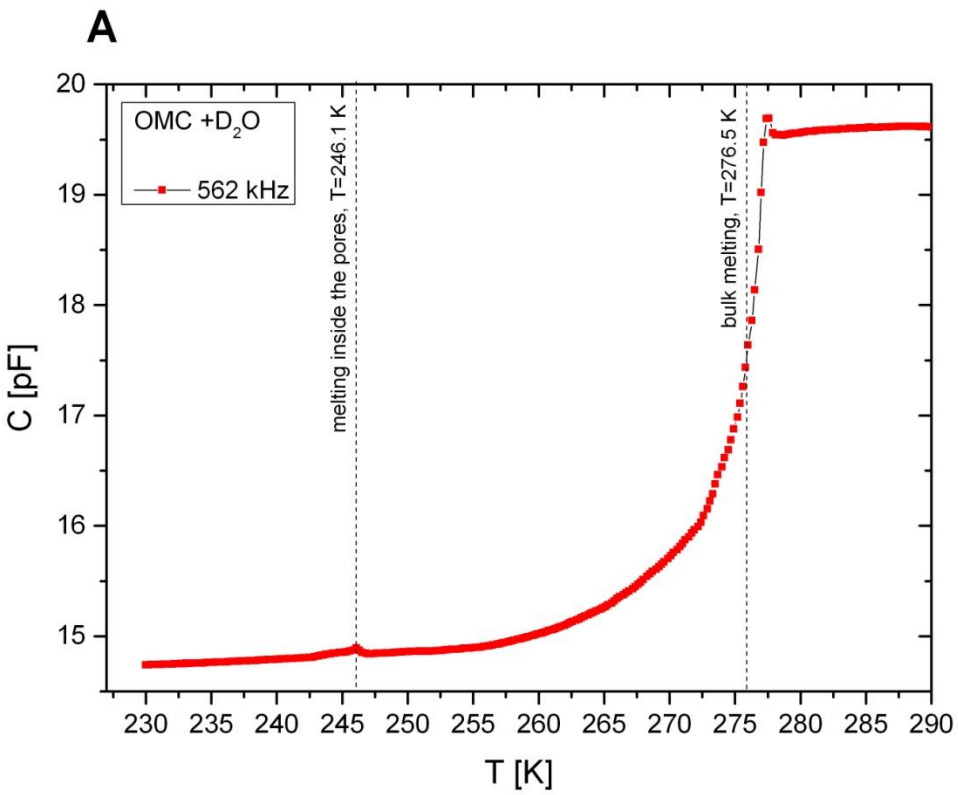

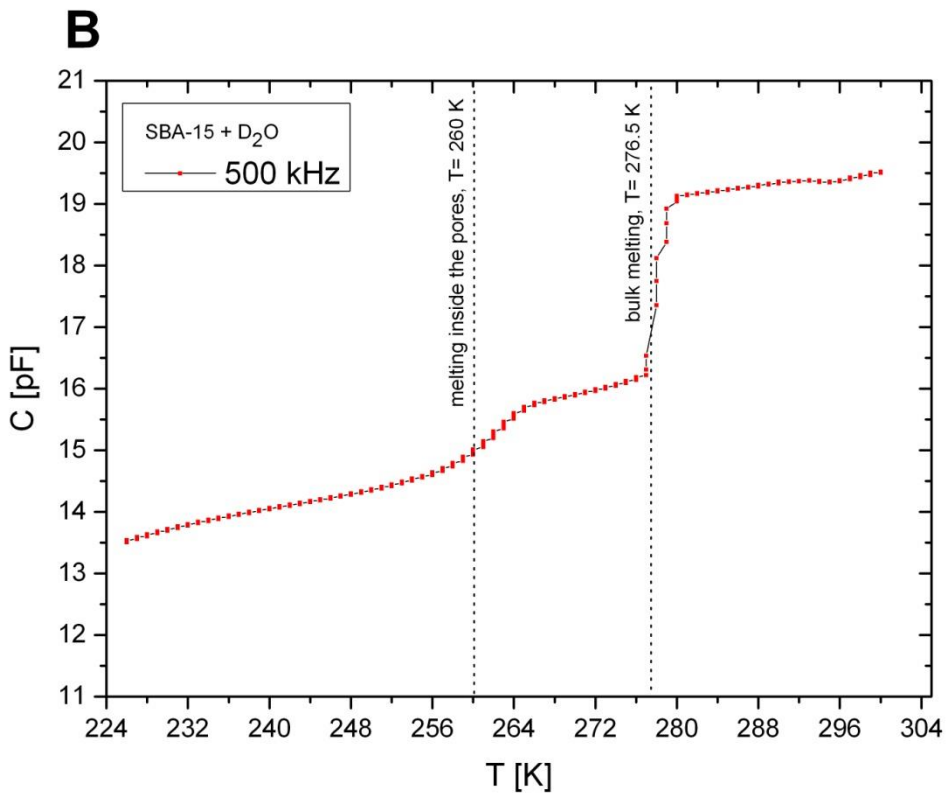

Table

Sample	Surface area (S_{BET})[a] (m^2/g)		Pore volume (cm^3/g)		Pore Size distribution (nm)		
	S_{Total}	S_{mic}[b]	V_{Total}[c]	V_{mic}[b]	D_h[d]	$D_{mo\ (NLDFT)}$[e]	$D_{mo\ (BJH)}$[f]
OMC	757	23	0.87	0.006	4.6	0.4	3.9
SBA-15	460	16	0.6	0.004	5.3	*	5.5

Name of Material/ Equipment	Company	Catalog Number
1,3,5-trimethylbenzene	Sigma-Aldrich, Poland	M7200 Sigma-Aldrich
anhydrous ethanol	POCH, Avantor Performance Materials Poland S.A.	396480111
ASAP 2020. Accelerated Surface Area and Porosimetry System	Micromeritics Instrument Corporation, Norcross, GA, USA	
Automatic burette Dosimat 665	Metrohm, Switzerland	
Digital pH-meter pHm-240	Radiometer, Copenhagen	
ethyl alcohol	POCH, Avantor Performance Materials Poland S.A.	396420420
glucose	POCH, Avantor Performance Materials Poland S.A.	459560448
Hydrochloric acid	POCH, Avantor Performance Materials Poland S.A.	575283115

HOPG graphite substrate	Spi Supplies	LOT#1170906
Impedance analyzer Solartron 1260	Solartron	
Pluronic PE 6400 polymer	BASF (Polska)	
Pluronic PE10500	BASF Canada Inc.	
potassium hydroxide	Sigma-Aldrich, Poland	P5958 Sigma-Aldrich
SEM microscope	JEOL JSM-7001F	
Sigma Force Tensiometer 701	KSV, Sigma701, Biolin Scientific	
Sulfuric acid (VI)	POCH, Avantor Performance Materials Poland S.A.	575000115
surface glass type KS 324 Kavalier	Megan Poland	
Tecnai G2 T20 X-TWIN	FEI, USA	
TEM microscope	JEOL JEM-1400	
temperature controller ITC503	Oxford Instruments	
Tetraethylorthosilicate	Sigma-Aldrich, Poland	131903
Ultrapure water	Millipore, Merck KGaA, Darmstadt, Germany	SIMSV0001

Comments/Description

Mesitylene, also known as 1,3,5-trimethylbenzene, reagent grade, assay: 98%.

Assay, min. 99.8 %, analysis-pur (a.p.)

Samples were outgassed before analysis at 120 ^{o}C for 24 hours in degas port of analyzer. The dead space volume was measured for calibration on experimental measurement using helium as a adsorbate.

The surface charge properties were experimentally determined by potentiometric titration of the suspension at constant temperature 20°C maintained by the thermostatic device. Prior to potentiometric titration measurements, the solid samples were dried by 24 hours at 120 ^{o}C. The initial pH was established by addition of 0.3 cm^3 of 0.2 mol/L HCl. T The 0.1 mol/L NaOH solution was used as a titrant, added gradually by using automatic burette.

Device coupled with automatic burette

Assay, min. 96 %.analysis-pur (a.p.)

assay 99.5%

Hydrochloric acid, 35 - 38% analysis-pur (a.p.)

HOPG SPI-2 Grade, 20x20x1 mm

($EO_{13}PO_{70}EO_{13}$)
Molar mass 6500 g/mol
BioXtra, ≥85% KOH basis
Scanning Electron Microscope with EDS detector

force tensiometer

80 % of SiO2 , 11% of Na2O and 9% of CaO
Transmission Electron Microscope with EDX detector.

Tetraethyl silicate, TEOS, reagent grade, assay 98%

Simplicity Water Purification SystemUltrapure Water: 18.2 MegOhm·cm, TOC: <5 ppb

ARTICLE AND VIDEO LICENSE AGREEMENT

Title of Article: Surface properties of synthesized nanoporous carbon and silica matrices; the melting of D_2O confined inside these pores

Author(s): A. Stevczyńska, M. Zientkiewicz-Strońska, A. Derjo-Horodecka, M. Sliwińska-Bartkowiak

Item 1: The Author elects to have the Materials be made available (as described at http://www.jove.com/publish) via:

☑ Standard Access ☐ Open Access

Item 2: Please select one of the following items:

☑ The Author is **NOT** a United States government employee.

☐ The Author is a United States government employee and the Materials were prepared in the course of his or her duties as a United States government employee.

☐ The Author is a United States government employee but the Materials were NOT prepared in the course of his or her duties as a United States government employee.

ARTICLE AND VIDEO LICENSE AGREEMENT

1. **Defined Terms.** As used in this Article and Video License Agreement, the following terms shall have the following meanings: "**Agreement**" means this Article and Video License Agreement; "**Article**" means the article specified on the last page of this Agreement, including any associated materials such as texts, figures, tables, artwork, abstracts, or summaries contained therein; "**Author**" means the author who is a signatory to this Agreement; "**Collective Work**" means a work, such as a periodical issue, anthology or encyclopedia, in which the Materials in their entirety in unmodified form, along with a number of other contributions, constituting separate and independent works in themselves, are assembled into a collective whole; "**CRC License**" means the Creative Commons Attribution-Non Commercial-No Derivs 3.0 Unported Agreement, the terms and conditions of which can be found at: http://creativecommons.org/licenses/by-nc-nd/3.0/legalcode; "**Derivative Work**" means a work based upon the Materials or upon the Materials and other pre-existing works, such as a translation, musical arrangement, dramatization, fictionalization, motion picture version, sound recording, art reproduction, abridgment, condensation, or any other form in which the Materials may be recast, transformed, or adapted; "**Institution**" means the institution, listed on the last page of this Agreement, by which the Author was employed at the time of the creation of the Materials; "**JoVE**" means MyJove Corporation, a Massachusetts corporation and the publisher of The Journal of Visualized Experiments; "**Materials**" means the Article and / or the Video; "**Parties**" means the Author and JoVE; "**Video**" means any video(s) made by the Author, alone or in conjunction with any other parties, or by JoVE or its affiliates or agents, individually or in collaboration with the Author or any other parties, incorporating all or any portion of the Article, and in which the Author may or may not appear.

2. **Background.** The Author, who is the author of the Article, in order to ensure the dissemination and protection of the Article, desires to have the JoVE publish the Article and create and transmit videos based on the Article. In furtherance of such goals, the Parties desire to memorialize in this Agreement the respective rights of each Party in and to the Article and the Video.

3. **Grant of Rights in Article.** In consideration of JoVE agreeing to publish the Article, the Author hereby grants to JoVE, subject to **Sections 4** and **7** below, the exclusive, royalty-free, perpetual (for the full term of copyright in the Article, including any extensions thereto) license (a) to publish, reproduce, distribute, display and store the Article in all forms, formats and media whether now known or hereafter developed (including without limitation in print, digital and electronic form) throughout the world, (b) to translate the Article into other languages, create adaptations, summaries or extracts of the Article or other Derivative Works (including, without limitation, the Video) or Collective Works based on all or any portion of the Article and exercise all of the rights set forth in (a) above in such translations, adaptations, summaries, extracts, Derivative Works or Collective Works and(c) to license others to do any or all of the above. The foregoing rights may be exercised in all media and formats, whether now known or hereafter devised, and include the right to make such modifications as are technically necessary to exercise the rights in other media and formats. If the "Open Access" box has been checked in **Item 1** above, JoVE and the Author hereby grant to the public all such rights in the Article as provided in, but subject to all limitations and requirements set forth in, the CRC License.

jove

ARTICLE AND VIDEO LICENSE AGREEMENT

4. **Retention of Rights in Article.** Notwithstanding the exclusive license granted to JoVE in **Section 3** above, the Author shall, with respect to the Article, retain the non-exclusive right to use all or part of the Article for the non-commercial purpose of giving lectures, presentations or teaching classes, and to post a copy of the Article on the Institution's website or the Author's personal website, in each case provided that a link to the Article on the JoVE website is provided and notice of JoVE's copyright in the Article is included. All non-copyright intellectual property rights in and to the Article, such as patent rights, shall remain with the Author.

5. **Grant of Rights in Video – Standard Access.** This **Section 5** applies if the "Standard Access" box has been checked in **Item 1** above or if no box has been checked in **Item 1** above. In consideration of JoVE agreeing to produce, display or otherwise assist with the Video, the Author hereby acknowledges and agrees that, Subject to **Section 7** below, JoVE is and shall be the sole and exclusive owner of all rights of any nature, including, without limitation, all copyrights, in and to the Video. To the extent that, by law, the Author is deemed, now or at any time in the future, to have any rights of any nature in or to the Video, the Author hereby disclaims all such rights and transfers all such rights to JoVE.

6. **Grant of Rights in Video – Open Access.** This **Section 6** applies only if the "Open Access" box has been checked in **Item 1** above. In consideration of JoVE agreeing to produce, display or otherwise assist with the Video, the Author hereby grants to JoVE, subject to **Section 7** below, the exclusive, royalty-free, perpetual (for the full term of copyright in the Article, including any extensions thereto) license (a) to publish, reproduce, distribute, display and store the Video in all forms, formats and media whether now known or hereafter developed (including without limitation in print, digital and electronic form) throughout the world, (b) to translate the Video into other languages, create adaptations, summaries or extracts of the Video or other Derivative Works or Collective Works based on all or any portion of the Video and exercise all of the rights set forth in (a) above in such translations, adaptations, summaries, extracts, Derivative Works or Collective Works and (c) to license others to do any or all of the above. The foregoing rights may be exercised in all media and formats, whether now known or hereafter devised, and include the right to make such modifications as are technically necessary to exercise the rights in other media and formats. For any Video to which this **Section 6** is applicable, JoVE and the Author hereby grant to the public all such rights in the Video as provided in, but subject to all limitations and requirements set forth in, the CRC License.

7. **Government Employees.** If the Author is a United States government employee and the Article was prepared in the course of his or her duties as a United States government employee, as indicated in **Item 2** above, and any of the licenses or grants granted by the Author hereunder exceed the scope of the 17 U.S.C. 403, then the rights granted hereunder shall be limited to the maximum rights permitted under such statute. In such case, all provisions contained herein that are not in conflict with such statute shall remain in full force and effect, and all provisions contained herein that do so conflict shall be deemed to be amended so as to provide to JoVE the maximum rights permissible within such statute.

8. **Protection of the Work.** The Author(s) authorize JoVE to take steps in the Author(s) name and on their behalf if JoVE believes some third party could be infringing or might infringe the copyright of either the Author's Article and/or Video.

9. **Likeness, Privacy, Personality.** The Author hereby grants JoVE the right to use the Author's name, voice, likeness, picture, photograph, image, biography and performance in any way, commercial or otherwise, in connection with the Materials and the sale, promotion and distribution thereof. The Author hereby waives any and all rights he or she may have, relating to his or her appearance in the Video or otherwise relating to the Materials, under all applicable privacy, likeness, personality or similar laws.

10. **Author Warranties.** The Author represents and warrants that the Article is original, that it has not been published, that the copyright interest is owned by the Author (or, if more than one author is listed at the beginning of this Agreement, by such authors collectively) and has not been assigned, licensed, or otherwise transferred to any other party. The Author represents and warrants that the author(s) listed at the top of this Agreement are the only authors of the Materials. If more than one author is listed at the top of this Agreement and if any such author has not entered into a separate Article and Video License Agreement with JoVE relating to the Materials, the Author represents and warrants that the Author has been authorized by each of the other such authors to execute this Agreement on his or her behalf and to bind him or her with respect to the terms of this Agreement as if each of them had been a party hereto as an Author. The Author warrants that the use, reproduction, distribution, public or private performance or display, and/or modification of all or any portion of the Materials does not and will not violate, infringe and/or misappropriate the patent, trademark, intellectual property or other rights of any third party. The Author represents and warrants that it has and will continue to comply with all government, institutional and other regulations, including, without limitation all institutional, laboratory, hospital, ethical, human and animal treatment, privacy, and all other rules, regulations, laws, procedures or guidelines, applicable to the Materials, and that all research involving human and animal subjects has been approved by the Author's relevant institutional review board.

11. **JoVE Discretion.** If the Author requests the assistance of JoVE in producing the Video in the Author's facility, the Author shall ensure that the presence of JoVE employees, agents or independent contractors is in accordance with the relevant regulations of the Author's institution. If more than one author is listed at the beginning of this Agreement, JoVE may, in its sole

jove

ARTICLE AND VIDEO LICENSE AGREEMENT

discretion, elect not take any action with respect to the Article until such time as it has received complete, executed Article and Video License Agreements from each such author. JoVE reserves the right, in its absolute and sole discretion and without giving any reason therefore, to accept or decline any work submitted to JoVE. JoVE and its employees, agents and independent contractors shall have full, unfettered access to the facilities of the Author or of the Author's institution as necessary to make the Video, whether actually published or not. JoVE has sole discretion as to the method of making and publishing the Materials, including, without limitation, to all decisions regarding editing, lighting, filming, timing of publication, if any, length, quality, content and the like.

12. **Indemnification.** The Author agrees to indemnify JoVE and/or its successors and assigns from and against any and all claims, costs, and expenses, including attorney's fees, arising out of any breach of any warranty or other representations contained herein. The Author further agrees to indemnify and hold harmless JoVE from and against any and all claims, costs, and expenses, including attorney's fees, resulting from the breach by the Author of any representation or warranty contained herein or from allegations or instances of violation of intellectual property rights, damage to the Author's or the Author's institution's facilities, fraud, libel, defamation, research, equipment, experiments, property damage, personal injury, violations of institutional, laboratory, hospital, ethical, human and animal treatment, privacy or other rules, regulations, laws, procedures or guidelines, liabilities and other losses or damages related in any way to the submission of work to JoVE, making of videos by JoVE, or publication in JoVE or elsewhere by JoVE. The Author shall be responsible for, and shall hold JoVE harmless from, damages caused by lack of sterilization, lack of cleanliness or by contamination due to the making of a video by JoVE its employees, agents or independent contractors. All sterilization, cleanliness or decontamination procedures shall be solely the responsibility of the Author and shall be undertaken at the Author's expense. All indemnifications provided herein shall include JoVE's attorney's fees and costs related to said losses or damages. Such indemnification and holding harmless shall include such losses or damages incurred by, or in connection with, acts or omissions of JoVE, its employees, agents or independent contractors.

13. **Fees.** To cover the cost incurred for publication, JoVE must receive payment before production and publication of the Materials. Payment is due in 21 days of invoice. Should the Materials not be published due to an editorial or production decision, these funds will be returned to the Author. Withdrawal by the Author of any submitted Materials after final peer review approval will result in a US$1,200 fee to cover pre-production expenses incurred by JoVE. If payment is not received by the completion of filming, production and publication of the Materials will be suspended until payment is received.

14. **Transfer, Governing Law.** This Agreement may be assigned by JoVE and shall inure to the benefits of any of JoVE's successors and assignees. This Agreement shall be governed and construed by the internal laws of the Commonwealth of Massachusetts without giving effect to any conflict of law provision thereunder. This Agreement may be executed in counterparts, each of which shall be deemed an original, but all of which together shall be deemed to me one and the same agreement. A signed copy of this Agreement delivered by facsimile, e-mail or other means of electronic transmission shall be deemed to have the same legal effect as delivery of an original signed copy of this Agreement.

A signed copy of this document must be sent with all new submissions. Only one Agreement is required per submission.

CORRESPONDING AUTHOR

Name:	Małgorzata Śliwińska-Bartkowiak
Department:	Physics' Faculty
Institution:	A. Mickiewicz University, Poznań, Poland
Title:	Professor
Signature:	Małgorzata Śliwińska-Bartkowiak
Date:	31.08.2018

Please submit a **signed** and **dated** copy of this license by one of the following three methods:

1. Upload an electronic version on the JoVE submission site
2. Fax the document to +1.866.381.2236
3. Mail the document to JoVE / Attn: JoVE Editorial / 1 Alewife Center #200 / Cambridge, MA 02140

 For questions, please contact us at submissions@jove.com or +1.617.945.9051.

List of changes in the revised manuscript and detailed responses on the editorial comments

Editorial comments:

1. Please take this opportunity to thoroughly proofread the manuscript to ensure that there are no spelling or grammar issues. The JoVE editor will not copy-edit your manuscript and any errors in the submitted revision may be present in the published version.

Thank You for this comment. The text of manuscript was checked and improved.

2. Please revise lines 501-510, 517-518, 529-531, 533-536, 538-539, 540-541, 575-579 to avoid previously published text.

We agree with this remark. The lines were corrected following:
501-510 (now: 654-663): Two of an applied substrates are smooth and planar: silica and carbon surfaces, while the others have roughness and mesopores. The measured contact angles are discussed in relations to the microscopic wetting parameter, α_w. This parameter emerges from a corresponding states rule of the partition function for this system, and is a measure of the ratio between the liquid–pore walls intermolecular interactions to the interactions of two liquid molecules[22-24]. Therefore, this parameter is a well-defined measure of wettability at the nano- and macro-scales. The α_w parameter is shown to be a monotonic function of the contact angle. The results of measurements have found that contact angles for the rough surfaces were larger than those for the smooth planar surfaces for all studied liquids, including non-wetting and well-wetting liquids. These results suggest the Cassie-Baxter mechanism of wettability on nano-
517-518 (now: 686-687): f increases monotonically with an increase of α_w parameter, what confirms a Cassie–Baxter model of wetting on rough substrates.
529-531 (now: 698-700): temperature dependence of capacitance C shows a sharp increase at T=260 K, corresponding to the melting of adsorbed D_2O inside the pores of SBA-15 and at T=246.1 K, which refers to the melting of adsorbed water inside the pores of OMC. For both systems we observe the second
533-536 (now: 702-705): deuterated water. The observed signals come from both the bulk and the confined liquid, because the samples studied here are a suspension of filled porous matrices in the pure liquid. We can observe that the melting temperature of D_2O in SBA-15 pores is depressed relative to the temperature of the bulk by $\Delta T=T_{m,pore} - T_{m,bulk} =- 16.5$ K, while for OMC $\Delta T=- 30.4$ K.

538-539 (now: 707-708): literature the melting temperature in the pores $T_{m,pore}$ can be considered in terms of two variables: pore size H and wettability parameter α_w. For smaller α_w values ($\alpha_w << 1$) the
540-541 (now: 708-710): For smaller α_w values ($\alpha_w << 1$) the depression of $T_{m,pore}$ is expected. If the pore width H is the same, then the change in the α_w value of the system affects on the change of the $T_{m,pore}$.
575-579: Revised and moved from the Conclusion section partially to Results and Discussion section.

3. Please remove the embedded figure(s) from the manuscript.

The embedded figures were removed from the manuscript.

4. Figures: Please line up the panels better. Some panels are off-set in Figure. Please ensure

that the panels are of the same dimensions if possible. Please use consistent font size among panels in the same figure, if possible.

Thank You for this remark. The changes were implemented.

5. Please shorten the title if possible.

The title was shorten. Now the manuscript is titled: Surface properties of synthesized nanoporous carbon and silica matrices; the melting of D_2O confined inside these pores.

6. Please add a Long Abstract (150-300 word) before Introduction section. It should include a statement about the purpose of the method. A more detailed overview of the method and a summary of its advantages, limitations, and applications is appropriate. Please focus on the general types of results acquired.

The Long Abstract was added (lines: 34-54) (293 words).

7. Please rephrase the Introduction to include a clear statement of the overall goal of this method.

Thank You for the comment. The introduction was changed in following way:

Gas adsorption is one of major importance for the characterization of a wide range of porous materials. Of all the many gases and vapours, which are available and may be used as adsorptives, nitrogen has remained universally properties. With the aid of user-friendly commercial equipment and data processing, it is now possible to use nitrogen adsorption at 77 K to determine nitrogen adsorption–desorption isotherms at 77 K in a wide range of p/p_0. All the computational procedures for pore size analysis have limitations. The various assumptions include an ideal pore shape, rigidity of the structure and typical model (capillary condensation or micropore filling). The derived pore widths and pore volumes should be regarded as effective values with respect to the adsorption of nitrogen at 77 K. The surface characteristics related with surface chemistry of the materials depend on surface charge related with the heteroatoms or functional groups present on the surface. Measurements of the dielectric constant allow on the investigation of melting phenomena, as the polarizability of the liquid and solid phases are different from each other. A change in the slope of the temperature dependence of the capacitance shows that melting occurs in the system.

8. Please use SI abbreviations for all units: L, mL, µL, h, min, s, etc.

The SI abbreviations were used in the manuscript.

9. Please include a space between all numbers and their corresponding units: 15 mL, 37 °C, 60 s; etc.

We improved it, including the spaces.

10. Please remove all commercial language from your manuscript and use generic terms instead. All commercial products should be sufficiently referenced in the Table of Materials and Reagents. For example: Micromeritics Corp. Norcross, JEOL JEM-1400, JEOL JSM-7001F, KSV701, Solartron 1260, etc.

All commercial language were removed and putted in the Table of Materials and Reagents.

11. 3.1.1, 3.2.1, 3.3.1, 3.5.7, lines 295-297: Please write the text in the imperative tense as if telling someone how to do the technique (e.g., "Do this," "Ensure that," etc.).

We used the imperative tenses in given places.

12. 3.1.2: Please specify the mass of sample added.

The mass was specified in line 243:

3.1.4 Fill the tube with the sample, weighing the mass of the sample c.a. 0.20 g.

13. 3.1.4: What does it mean by weighing the mass of the sample from 0.15 g to 0.20 g? Please clarify.

The mass was specified in line 243:

3.1.4 Fill the tube with the sample, weighing the mass of the sample c.a. 0.20 g.

14. 3.1.5: Please describe how to degas the adsorbents.

The additional explanation was added:

Lines 245-248: Prior to the measurements, degas the adsorbents at 150 °C K for at least 24 hours. Glass tube with the sample place in degas port of ASAP analyzer. In the degassing port, the sample is connected to the vacuum (5µm Hg) and heated to the set temperature. After degassing, fill the sample with nitrogen and transfer to the analysis port.

15. 3.2.2: Please specify the sample mass and volume of ethanol added.

The lines 255-256 were changed:

3.2.2: In order to obtain a monodisperse film of the specimen, suspend 2-3 little grains of the sample in the 2 mL of ethanol and place in an ultrasonic bath for 3 h.

16. 3.3: Please change Elemental Analysis to Energy Dispersive X-Ray Spectroscopy.

Thank You for this remark. The title was changed (line 261).

17. 3.4.1: Please revise this sentence to be clear.

The additional explanation was added:
Lines 272-275: Potentiometric titration experiment perform by using an automatic burette, which

allows to the adding of titrant by small and controlled portions (according to the titration software and procedure). An automatic Dosimat should provide the smallest increment at least 1 µL.

18. Please revise to explain the Representative Results in the context of the technique you have described, e.g., how do these results show the technique, suggestions about how to analyze the outcome, etc.

The Representative Results were revised. The following explanations were added:

Lines 363-367: From the position of an inflection point on sorption isotherms (Fig. 1 (A), (C)), we receive an information about the pressure at which the process of mesopores filling starts; the knowledge of the value of pressure is needed for calculation of mean pore size and pores size distribution (PSD) (Fig. 1 (B), (D)), applying for this the Kelvin equation.

Lines 372-374: An interpretation of TEM images allows to an estimation of pore sizes and to comparison the values with the data obtained from sorption measurements (Fig. 1).

Lines 386-387: An analysis of position of zero charge point on pH scale provides an information about an acidity in the system. As the value of the pH pzc is lower, the sample is more acidic.

Lines 393-395: The value of energy of characteristic radiation coming from the sample allows to an identification of elements including in the studied sample, while the intensity (the height of the peaks in the spectrum) enables to an quantified analysis (Fig. 4 (C)).

Lines 412-416: The wettability determines the surface acidity; this method with the potentiometric titration and an EDX analysis constitutes the full description of the surface properties of the sample. As the value of contact angle is lower, then the wettability is better, what means that an interaction of penetrating liquid molecule is more pronounced with the studied surface (Fig. 5 (A) – (B)).

Lines 435-439: The dielectric results show the temperature dependences of electric capacity for both samples (Fig. 7 (A) – (B)). The anomalies visible in the C(T) curves evidence about phase transitions occurring in the system. The localization of the anomaly position allows to determine the melting point both: of the bulk liquid as well as the melting point in the pores of studied sample.

19. As we are a methods journal, please revise the Discussion to explicitly cover the following in detail in 3-6 paragraphs with citations:
a) Critical steps within the protocol
b) Any modifications and troubleshooting of the technique
c) Any limitations of the technique
d) The significance with respect to existing methods
e) Any future applications of the technique

The Discussion was revised. The following explanations were added:

Lines 511-529: The critical steps during preparation the ordered mesoporous carbon material include: preparation the ordered mesoporous silica materials as the template with well-defined structural properties that affect the property of the final materials and tempering/carbonization step under nitrogen atmosphere. The modification of the typical method of preparation the mesoporous

ordered silicates with cylindrical pores[28] concerned the application the not typical structure directing agent Pluronic PE10500 polymer for improving the structural properties of material. The 3D interconnected and stable porous structure of the template is necessary for preparation the mesoporous carbon materials. Moreover, a key disadvantage is the essential requirement of the sample treatment for the template removal. The properties of chemicals used in this step can affect the carbon surface and its functionality. The presented strategy propose the preparation the negative replication of OMCs based on ordered mesoporous solid template. The pore size control and symmetric ordering are simply determined using the silica template and is not associated with interaction between the carbon precursor and the template. The literature show the potential of OMC for various electrochemical systems[29-30]. The impregnation mechanism presented in this work, is responsible for facile process to precisely replicate the negative structure of the silica template. The nature of the hard template procedure ensures the pyrolysis phenomena causing less damage to the regular and ordered structure. Moreover, this method allows the easier graphitization of the OMC materials formed within the solid template.

Lines 543-554: The critical steps during nitrogen adsorption/desorption measurement include the very precise mass sample definition and sufficient degas step. The measurement procedure was performed according appropriate guidelines of this procedure. Despite the fact that physisorption measurements are widely used for the determination of surface area and pore size distribution, the interpretation of the experimental isotherms is not always straightforward. During the computation of the mesopore size distribution, by application the modified Kelvin equation (which is base of the theory) it is necessarily to accept the assumption of the rigid and of well-defined shape of pores. Moreover, the range of validity of the Kelvin equation and the interpretation of hysteresis loops on the isotherms remain still unresolved problems. The possibility of facilitation are related to the application of empirical methods of isotherm analysis (e.g. the α_s-method[29-34]). However, this manner require to utilize adsorption data obtained with non-porous reference materials.

Lines 564-577: The properties of the pore-network structure based on physical adsorption/desorption analyses is fundamental to the characterization of nanopowders and nanomaterials. Nitrogen adsorption/desorption methods can be regarded as the first stage in the characterization of microporous and mesoporous solids. The method is in general applicable to samples of all classes of porous bodies or materials. This method allows to estimate the porous structures based on the shapes of isotherms and hysteresis loops directly from experimental measurement. The nitrogen adsorption/desorption next to the other methods of porous structure determination (liquid intrusion[35], Light, X-ray, and Neutron Scattering[36-37] and microscopy[32]) is the most important and useful technique due to the wide applicability and mutual comparability of results. Nitrogen is typical considered a standard adsorptive molecule for pore characterization by gas adsorption method. It is possible to use other types of molecules (carbon dioxide, krypton, argon) could be applied for obtaining new information about the sample and the characterization of microporous materials.

Lines 588-598: Transmission electron microscopy is a significant analytical technique in the physical, chemical and biological sciences; TEM finds application in cancer research, virology and materials science as well as in nanotechnology and semiconductor research. Transmission electron microscopy is capable of imaging at higher resolution than light microscopes, owing to the smaller de Broglie wavelength of electrons. This enables to capture the details thousands of times smaller than a

resolvable object seen in a light microscope. An image is formed from the interaction of the electrons with the sample as the beam is transmitted through the specimen. Therefore, one of the limitations of the method is that the specimen should be an ultrathin section less than 100 nm thick or a suspension on a grid. TEM can be modified into a scanning transmission electron microscope (STEM) by the addition of a system that rasters the beam across the sample to form the image, combined with suitable detectors.

Lines 604-621: The negatively charged sites increase the van der Waals interactions between the guest and host molecules on the SBA-15 surface improving the adsorption of the silica matrix. The critical steps during potentiometric titration measurement include the very precise addition the titrant to the suspension and ensuring their continuity of mixing. The potentiometric titration procedure was performed fully automatic for ensuring the most appropriate results. The important and unique step was also application of special software for controlling and calculations. The limitation of this method is the calibration step of the pH electrode and ensuring the stable atmosphere (for example nitrogen) and temperature. Potentiometric titration can be categorized as acid/base titration procedure. This technique requires measuring the voltage change during titrant addition steps. It provides an adaptable, affordable and highly accurate technique to achieve high purity which is essential to many fields, particularly pharmaceuticals and functional materials. Actual, exist a number of kinds of potentiometric titrations providing possibilities depending on the need for determining samples. Some of them include acid-base, redox, precipitation and complexometric techniques. Potentiometric titrations as automated systems ensure greater capacity for sample characterization. These features ensure the continued usefulness of potentiometric titrations methods in material chemistry.

Lines 645-650: EDX is one of the techniques, which determines the atomic composition of the specimen. It does not give chemical information (e.g. oxidation state, chemical bonds), like a XPS method. For quantitative analysis EDX is not suitable for light elements, e.g. like oxygen, where it can detect the presence of oxygen, but not the proper quantification. This method works only for thin layer (few microns or less) on the surface and it is quite sensible to contamination current on the specimen.

Lines 664-681: Moreover, the measured contact angle for several liquids inside silica and carbon nanopores, indicate the better wettability of the silica walls relatively to the carbon walls and an influence of the pore roughness on the fluid/wall interactions, which is much pronounced for silica than for carbon nanopores. The capillary rise method is the basis of some methods that are widely applied for the determination of contact angles as well as wettabilities of small particles and porous powder materials. For a flat solid surface, many common techniques, e.g. sessile drop and Wilhelmy plate can be applied for measuring contact angles. To determine contact angles of liquids on powders or porous materials, four conditions have to be satisfied for the process (i.e. Washburn's equation is derived based on these four assumptions): (1) steady state laminar flow, (2) no external pressure, (3) negligible gravitational force and (4) zero velocity of the liquid at the solid/liquid interface (no slip). By comparison, the hydrostatic pressure is much smaller than the capillary pressure, therefore, the liquid rising upward through the tube is primary contributed by the capillary pressure. However, the wettability studies of small particles have always been critical in terms of precision and reproducibility of results. By taking into account the pressure increment and the hydrostatic effects in Washburn equation, it is theoretically possible to derive an improved

expression for capillary rise, in order to more accurately describe the relation between the pressure increment and time, which enables to experimentally measure contact angle of small particles precisely.

Lines 715-733: The obtained results have indicated an improvement of adhesion effects on the porous silica wall relative to the carbon wall. This method in relation to the studied sample has some limitations. One of them comes from the fact that the samples contain the signal from both: the bulk and the liquid confined in the pores. Therefore, the signal from the confined liquid is often weak and it is difficult to precisely determine the melting temperature. In the future is worth to simultaneously applying another method, e.g. differential scanning calorimetry with slow heating rate or to centrifuge of the sample from the excess liquid. Moreover, in the case of conductive samples, there is a need to use of teflon plate; then above the temperature of 250 K the signal is characterized by an increase, what results from the temperature dependence of electric capacity of teflon material. An advantage of dielectric spectroscopy method is a fact that the method is applied in many fields of research. For solutions far from glass transition, the time scale for molecular motions is in the order of tens of femtoseconds to nanoseconds, so that experiments should be conducted at frequencies in the MHz to THz region. In many aspects, such as the decomposition of the spectra or the interpretation and quantitative analysis of spectral contributions, the technique resembles more conventional spectroscopies. Differences lie in the selectivity—DRS detects the collective fluctuations of species having a permanent dipole moment and a sufficient life time. For example, infrared spectroscopy provides complementary information, although the sensitivity toward collective modes may complicate the interpretation of dielectric spectra.

20. JoVE article does not have a Conclusion section. Please move information in the Conclusion section to Results or Discussion section.

A conclusion section was moved partially to Results and partially to the Discussion section.

21. References: Please do not abbreviate journal titles. Please include volume and issue numbers for all references.

We improved the References. The journal titles were improved, volumes and issue numbers were added for all references.

List of changes in the revised manuscript and detailed responses to Reviewers

Reviewers' comments:

Reviewer #1:

Manuscript Summary:

The author reports the synthesis and characterization of the ordered mesoporous carbon material (OMC) and ordered silica porous matrix SBA-15. They describe the surface properties of mesoporous molecular sieves, their wettability, and the melting behavior of D2O confined in the different ordered porous materials with the similar pore sizes. It is an interesting work which can supply some reference to application of this kind of materials in catalysis or adsorption. The work is well study and written. I think it can be improved if the author can get directly evidence to support the conclusion by using some microtechnique.

Thank You for this comment. The Conclusion section was moved partially in the body of the Results and Discussion. As the examples of these microtechniques, we can indicate differential scanning calorimetry (DSC), where it would be a supplement of the used by us DS method. XPS microtechnique could be indicate the presence of the functional groups on the surface of molecular sieves.

Reviewer #2:

This JOVE manuscript describes the synthesis of a mesoporous silica material, similar to the original SBA-15 synthesis along followed by using this material to template the synthesis of ordered mesoporous carbon. The authors characterized the textural properties (nitrogen sorption), wettability, and melting behavior of D2O in the pores.

1. Reviewer's comment:

Why do the authors use the term "mesoporous" throughout the manuscript but use "nanoporous" in the title? This could be confusing for readers. The measured pore sizes for both materials are in the defined mesoporous range so this term should be consistently used.

Thank You for this suggestion, the "nanoporous" term was used in the whole manuscript. Additional information about the type of materials was introduced in the short abstract:

Line 28: We report the synthesis and characterization of the ordered nanoporous carbon material (called also ordered mesoporous carbon material (OMC)) with the pore size of 4.6 nm and ordered silica porous matrix: SBA-15 with the pore size of 5.3 nm of diameter.

2. Reviewer's comment:

Please use more description on the "dropwise" addition of TEOS, including how long the dropwise addition should take.

Additional explanations were added in the preparation step (lines 135-137):

1.1.5. After 30 minutes, add the 34 g of tetraethylorthosilicate (TEOS) to the flask. The TEOS addition perform slowly and dropwise while stirring constantly. The drop of whole quantity of TEOS should take 10 min.

3. Reviewer's comment:

Line 193 should be "Nitrogen Sorption" not "Nitrogen Adsorption" to be inclusive of the desorption measurements.

The more appropriate name of the technique was applied (line 230):

3.1. Low-temperature Nitrogen Adsorption/Desorption measurements.

4. Reviewer's comment:

Why is the tube filled up with "compressed nitrogen" during the prep for the nitrogen sorption analysis?

The filling the glass tube by compressed nitrogen was performed for minimize the weight error. The low-temperature nitrogen adsorption-desorption measurements were performed under nitrogen atmosphere, so the weighing the empty glass tube before the measurement should take place under the same conditions. For clarity, the description of this part of the experiment has been rewritten. (lines 232-248):

3.1.1 N_2 adsorption/desorption isotherms at 77 K are studied using an ASAP 2020 analyzer (Micromeritics Corp. Norcross, GA, USA).

3.1.2 Use appropriate glass tube for nitrogen sorption measurements. Before to put the porous sample in the glass tube, clean the tube in an ultrasonic washer and rinse with the bi-distilled water and with an anhydrous ethanol.

3.1.3 Heat the glass tube in an oven at 150 °C for 3 hours and fill up the tube with the compressed nitrogen. The weighing the empty glass tube before the measurement should take place under the nitrogen conditions for minimize the weight error.

3.1.4 Fill the tube with the sample, weighing the mass of the sample c.a. 0.20 g.

3.1.5 Prior to the measurements, degas the adsorbents (0.01 mmHg) at 423 K for 24 h. Glass tube with the sample place in degas port of ASAP analyzer. In the degassing port, the sample is connected to the vacuum (5μm Hg) and heated to the set temperature. After degassing, fill the sample with nitrogen and transfer to the analysis port.

5. Reviewer's comment:

3.2.2. These samples are not "dissolving" in ethanol for the TEM grid prep, they are being suspended.

We agree with this suggestion. It was corrected (line 255).

6. Reviewer's comment:

The value given for the work of wettability of OMC on line 544 is wrong.

We have calculated the value again and in our opinion it is correct. The work of immersed wettability in pores $W_e=\gamma_l \cos\theta_p$; if we substitute the obtained value of contact angle in the pores of OMC for D_2O equal $\theta_p=86.6$ ° and if we take the surface tension of D_2O equal 71.72 [mN/m], we will obtain the same result, i.e. $W_e=4,2432$ [mN/m]. Optionally, it might be approximated to the value $W_e=4.2$ [mN/m].

7. Reviewer's comment:

EDS by nature is not a quantitative measurement, authors need to be careful in making quantitative claims based off of EDS results.

We agree with this suggestion. Nevertheless, TEM/EDS analysis for identify the elements present in the sample can give the indicative quantitative analysis. In this case the differences between

carbon and oxygen content were significate and sufficient to establish the conclusions about the hydrophilicity of the carbon surface. Some improvements were incorporated in the text:

Lines 635-645: TEM-EDS spectra images of OMC surface from two different areas of sample are displayed in Figure 4(A) and 4(B). Oxygen and silicon atoms from the OMC surface were detected despite the predominant amount of carbon. The atomic and weight percentage of the elements are presented as insets. The atomic and weight percentage values of all elements obtained from different areas of the samples are similar and indicate about 98% of carbon content and only slightly more than 1 percent of the composition attributable to the oxygen. EDS microanalysis may suggest that the basic character of OMC surface is associated with the very low amount of oxygen-containing functional groups, which are typically predominantly of acidic functionality. Moreover, the basic functional groups can be responsible for the growing of hydrophilicity of the carbon materials. An EDS spectrum of silica matrix confirms the main contribution of oxygen and silicon abundance in the SBA-15 (Fig. 4 (C)).

8. Reviewer's comment:

Line 484, "Transition electron microscopy" is wrong

We agree with this suggestion. It was corrected. We put "Transmission electron microscopy" in the text.

9. Reviewer's comment:

On Page 5 the authors describe the results that are presented in Figure 5. The authors claim this result is indicative the "inside of the pores". It is not clear how the authors are certain they are measuring the wettability inside the pores.

We agree with the comment. The paragraph 3.5.1 was improved following:

3.5.1 In order to determine the contact angle inside the pores of studied samples, use the capillary rise method, based on the measurement of the mass rise of the liquid, which is penetrating the porous bed, as the function of the time. **The main assumption of this method is based on the fact that penetrating liquid is advancing into the porous column and that this column is set of intergranular capillaries with a certain average radius. Thus, every relations derived for single capillary are valid for the layer of the porous powder. In a single vertical capillary the wetting liquid floats against the gravitational forces as a result of the difference of pressures between the liquid and the vapor in the pores (capillary pressure). In this meaning, the penetration of the liquid into the porous bed allows to determine the dynamic advancing contact angle inside the pores.**

We applied the modified Washburn equation (Eqn. 2) to determine the value of contact angles inside the pores.

10. Reviewer's comment:

Don't use yellow in the figures in Figure 1, it is too difficult to see.

The color in the Fig.1 was changed on green.

11. Reviewer's comment:

This manuscript in its current form is not publishable. It would behoove the authors to seek out a native English speaking individual to assist in final editing and proofreading the manuscript.

The text was improved and corrected.

List of changes in the revised manuscript and detailed responses on the editorial comments

Editorial comments:

1. Please take this opportunity to thoroughly proofread the manuscript to ensure that there are no spelling or grammar issues.

Thank You for this comment. The text of manuscript was checked and improved.

2. The Short Abstract is over 50 word limit.

The Short Abstract was limited to 51 words in the following way:

We report the synthesis and characterization of ordered nanoporous carbon with the pore size of 4.6 nm and SBA-15 material with the pore size of 5.3 nm. The work describes the surface and textural properties of nanoporous molecular sieves, their wettability, and the melting behavior of D_2O confined in the materials.

3. JoVE cannot publish manuscripts containing commercial language. This includes company names of an instrument or reagent. Please remove all commercial language from your manuscript and use generic terms instead. All commercial products should be sufficiently referenced in the Table of Materials and Reagents. Examples of commercial language in your manuscript include Pluronic, Micromeritics Corp, ASAP, etc.

All commercial language were removed and putted in the Table of Materials and Reagents.

4. Please use h, min, s for time units.

The SI abbreviations were used in the manuscript.

5. Step 3.1.1: Please write this step in the imperative tense.

The imperative tense was used and the step 3.1.1 was improved.

6. 3.1.5: Please ensure that all text is written in imperative tense.

We used the imperative tenses in given place.

7. 3.2.1: Please write this step in the imperative tense.

The imperative tense was used and the step 3.2.1 was improved.

8. 3.3.1: Please write this step in the imperative tense.

The imperative tense was used and the step 3.3.1 was improved.

9. 3.4.1: Please write this step in the imperative tense.

The imperative tense was used and the step 3.4.1 was improved.

10. 3.5.1, 3.5.2: These two steps cannot be filmed. Please do not highlight.

The two steps are not highlighted.

11. 3.5.7: This step cannot be filmed. Please do not highlight.

The step 3.5.7 is not highlighted.

12. Please remove the embedded figure(s) from the manuscript. All figures should be uploaded separately to your Editorial Manager account. Each figure must be accompanied by a title and a description after the Representative Results of the manuscript text.

The embedded figures (Figs. 1) were removed from manuscript body. Each figure is accompanied by a title and a description after the Representative Results of the manuscript text.

13. For each figure, please provide a title and a short description in the figure legend.

For each figure, a title and a short description was provided. Legends were included as part of the manuscript and were put in lines 442-480.

14. Please print and sign the attached Author License Agreement (ALA). Please then scan and upload the signed ALA with the manuscript files to your Editorial Manager account.

The attached Author License Agreement (ALA) was printed, signed and uploaded with the manuscript files to Editorial Manager account.

List of changes in the revised manuscript and detailed responses on the editorial comments

Editorial comments:

1. Unfortunately, there are a few sections of the manuscript that show significant overlap with previously published work. Though there may be a limited number of ways to describe a technique, please use original language throughout the manuscript. Please check the iThenticateReport attached to this email and revise lines 52-55, line 99-108, line 562-572, line 576-580, line 628-638, line 644-657, line 673-683, line 703-712.

The text of manuscript was checked and the following changes were implemented:

lines 52-55: using dielectric method. The results have shown that the depression of the melting temperature of D_2O in the pores of OMC is higher about 15 K relative to the depression of the melting temperature in SBA-15 pores with the comparable size of 5 nm. This is caused by an influence of adsorbate/adsorbent interactions of the studied matrices.

line 99-108: Gas adsorption is one of the most important technique of the characterization of porous materials. From many available and used gases and vapours, nitrogen has remained universally properties as adsorptive. An application of user-friendly commercial equipment and data processing, allows to determine nitrogen adsorption–desorption isotherms at 77 K in a wide range of p/p_0. As all the computational procedures for pore size analysis, this method have also some limitations. There are some assumptions, such as: an ideal pore shape, rigidity of the structure and model of pores filling, e.g.: capillary condensation or micropore filling. The determined pore widths and volumes should take into account effective values with respect to the adsorption of nitrogen at 77 K.

line 562-572: Transmission electron microscopy is a far-reaching analytical technique in the physics, chemistry and biology sciences; TEM finds application in many areas, such as: cancer research, virology , materials science and also in nanotechnology and in semiconductor research. Transmission electron microscopy is able to image at higher resolution than light microscopy due to the smaller de Broglie wavelength of electrons. This enables to capture the details thousands of times smaller than a resolvable object seen in a light microscopy. Here, an image comes from an interaction of the electrons with the sample when the beam is transmitted throughout the specimen. Therefore, one of the limitations of the method is that the specimen should be an ultrathin film less than 100 nm of thickness or a suspension applied on a grid. TEM can be improved by a scanning transmission electron microscope (STEM). It should be possible by an addition of a system combined with suitable detectors, which will raster the beam across the sample to form the image.

line 576-580: Potentiometric titration results of SBA-15 material show the shift of pH_{pzc} towards lower pH values evidencing of the existence of some acid centers on the SBA-15 surface. The negatively charged sites increase the van der Waals interactions between the adsorbent/adsorbate molecules in the SBA-15 matrix improving the adsorptive properties of the silica matrix.

line 628-638: In Fig. 5(A) and 5(B) we present experimental results of the contact angle for several liquids on silica and carbon substrates; we can see that the systems concerns a wide range of wettabilities. Two of an applied substrates are smooth and planar: silica and carbon surfaces, while the others possess roughness and mesopores. The measured contact angles are discussed in meaning of the microscopic wetting parameter, α_w. This parameter is based on a corresponding states rule of the partition function for these systems, and is a measure of the ratio between the liquid–pore walls intermolecular interactions to the interactions of two liquid molecules[22-24]. Therefore, this parameter measures the wetting properties at the nano- and macro-scales. The α_w parameter is shown to be a monotonic function of a contact angle. The results of measurements have found that the values of contact angles for the surfaces with the roughness are higher than those for the smooth planar surfaces, irrespective of type of studied liquids, including non-wetting and well-wetting liquids.

line 644-657: used to the determine the contact angles and wettability of small particles in the powders. For a flat solid substrate, many widespread techniques such as: sessile drop method and Wilhelmy plate method can be practiced for measuring contact angles. Using of capillary rise method assumes the fulfillment of four conditions during the process (i.e. Washburn's equation is derived based on these four assumptions): (1) steady laminar flow, (2) lack of an external pressure, (3) negligible gravitational force and (4) lack of the movement of the liquid at the solid/liquid interface. The hydrostatic pressure is much smaller than the capillary pressure, therefore, the liquid rising upward along the tube is primary fostered by the capillary pressure. The wettability studies of small particles should always take in account the precision and reproducibility of results. To precisely measure contact angle of small particles, it should be consider the pressure increment and the hydrostatic effects in Washburn equation; it allows to more accurately describe the relation between the pressure increment and time.

line 673-683: of D_2O in SBA-15 and OMC, matrices with the comparable pores size of 5 nm, the dielectric method was used. The results of the electric capacity of water placed in OMC and SBA-15 for the heating process presented in Figure 7(A) and 7(B) respectively, indicate that, the temperature dependence of capacitance C shows a sharp increase at T=260 K, corresponding to the melting of adsorbed D_2O inside the pores of SBA-15 and at T=246.1 K, which refers to the melting of adsorbed water inside the pores of OMC. For both systems we observe an increase in the C(T) function at T=276.5 K, which is referred to the melting point of the bulk deuterated water. The observed signals are related with both the bulk and the confined liquid, because the samples studied here are a suspension of filled porous matrices in the excessed liquid. We report that the melting temperature of D_2O in SBA-15 pores is depressed relative to the temperature of the bulk by $\Delta T=T_{m,pore} - T_{m,bulk} = - 16.5$ K, while for OMC $\Delta T=- 30.4$ K.

line 703-712: spectroscopy method is a fact that the method has a rich use in many areas of research as glass transitions, the time-scale molecular motions, whose are in the order of tens of femtoseconds to nanoseconds, so that experiments should be conducted at frequencies in the MHz to THz range. In many problems, such as the decomposition of the obtained spectra or the interpretation and quantitative analysis of the results, the technique resembles more common spectroscopies. Differences lie in the selectivity—the dielectric method investigates the collective fluctuations of molecules having a permanent dipole moment (polar liquids) and having long life time. For example, infrared spectroscopy provides complementary information, although the sensitivity in the direction to collective modes may impede the interpretation of dielectric spectra.

2. The Short Abstract is over 50 word limit.

The Short Abstract was shorted to 50 words:

We report the synthesis and characterization of ordered nanoporous carbon with the pore size of 4.6 nm and SBA-15 with the pore size of 5.3 nm. The work describes the surface and textural properties of nanoporous molecular sieves, their wettability, and the melting behavior of D_2O confined in the materials.

3. Step 1.1.3: What's the temperature setting for heating?

The paragraph was changed following:

Place the flask in an ultrasonic bath. Heat the solution to 35 °C and stir it until solid polymer is completely dissolved and create homogeneous mixture.

4. 1.2.1: What's the concentration of sulfuric acid?

The paragraph was changed following:

Prepare impregnation solutions (IS1 and IS2) with appropriate proportions of water, 3 M sulfuric acid (VI) and glucose. Glucose plays a role of carbon precursor, and sulfuric acid acts as catalyst.

5. 2.1.3: What's the temperature setting for heating?

The paragraph was changed following:

Place the flask in an ultrasonic bath. Heat the solution to 40 °C and stir it until solid polymer is completely dissolved and create homogeneous mixture (about 30 min).

6. 3.5.1: Please ensure that all text is written in imperative tense. Any text that cannot be written in the imperative tense may be added as a "Note."

The paragraph was improved. All text that cannot be written in imperative tense, was putted as a "Note":

Lines: 298-306: Note: This method is based on the measurement of the mass rise of the liquid, which is penetrating the porous bed, as the function of the time. The main assumption of this method is based on the fact that penetrating liquid is advancing into the porous column and that this column is set of intergranular capillaries with a certain average radius. Thus, every relations derived for single capillary are valid for the layer of the porous powder. In a single vertical capillary the wetting liquid floats against the gravitational forces as a result of the difference of pressures between the liquid and the vapor in the pores (capillary pressure). In this meaning, the penetration of the liquid into the porous bed allows to determine the dynamic advancing contact angle inside the pores.

7. 3.6.1: Please ensure that all text is written in imperative tense. Any text that cannot be written in the imperative tense may be added as a "Note."

The paragraph was improved. All text that cannot be written in imperative tense, was putted as a "Note":

Lines: 350-352: Note: The complex electric permittivity is defined as $\varepsilon^*=\varepsilon`+i\varepsilon``$, where $\varepsilon`=C/C_0$ is the real, and $\varepsilon``= tg\delta \cdot \varepsilon`$ is an imaginary part of the permittivity, where C_0 is the capacitance in the absence of the dielectric medium and tgδ are the dielectric losses.

8. Figure 1: Please add a short description of the figure in addition to the figure title in the figure legend.

A short description of the Figure 1 was added in the figure legend:

The nitrogen isotherms show characteristic hysteresis loops providing an information about the shape and pore size distributions of the studied pores.

9. Figure 3: Please add a short description of the figure in addition to the figure title in the figure legend.

A short description of the Figure 3 was added in the figure legend:

The surface charge density dependence of pH show the differences in electrochemical character of both materials; the value of the pzc point evidences about the acid sites existing in the sample.

10. Figure 4: Please add a short description of the figure in addition to the figure title in the figure legend.

A short description of the Figure 4 was added in the figure legend:

A quantitative results of EDS analysis allows to describe if the studied surface has the elements related with the functional groups responsible for its reactivity; this is a complementary technique for the potentiometric titration.

11. Figure 5: Please add a short description of the figure in addition to the figure title in the figure legend.

A short description of the Figure 5 was added in the figure legend:

The wettability inside the pores referred to the wettability on flat surfaces provides some information about the adsorbate/adsorbent interactions.

12. Figure 6: Please add a short description of the figure in addition to the figure title in the figure legend.

A short description of the Figure 6 was added in the figure legend:

An application of Cassie-Baxter model of wettability allows to interpretation of contact angles on rough porous substrates. The calculated from this model f fractions describe the percent contributions of porous wall which are in direct contact with liquid area.

13. Figure 7: Please add a short description of the figure in addition to the figure title in the figure legend.

A short description of the Figure 7 was added in the figure legend:

An interpretation of C(T) function allows to localize the temperature of phase transition occurring in the studied system. An increase of C(T) function evidences about the melting point for both: bulk water and confined water inside the pores. The value of the melting point shift is dependent on the host/guest molecular interactions.

List of changes in the revised manuscript

1. Please employ professional copy-editing services as the language in the manuscript is very difficult to read, especially the Representative Results and the Discussion.

The text of the manuscript was checked and the language was improved in the all body of the manuscript, with particular emphasis on the Representative Results and the Discussion section.

2. Please revise the following lines to avoid plagiarized text: 95-98, 101-103, 366-368, 523-525, 658-660, 691-693, 710-714:

The text of manuscript was checked and the following changes were implemented:

lines 95-98 and lines 101-103:

Low temperature gas adsorption/desorption measurement is one of the most important technique during the characterization of porous materials. Nitrogen gas is used as adsorbate molecules due to its high purity and possibility for creating strong interaction with solid adsorbents. Important advantages of this technique are: user-friendly commercial equipment and relatively easy data processing procedures. Determination of nitrogen adsorption/desorption isotherms based on accumulation the adsorbate molecules on the surface of solid adsorbent at 77 K in a wide range of pressure (p/p_0). The Barrett, Joyner, and Halenda (BJH) procedure for calculating pore size distribution from experimental adsorption or desorption isotherms was applied. The most important assumptions of BJH method include a planar surface and evenly distribution of the adsorbate on the investigated surface. However, this theory are based on the Kelvin equation and it still remains the most widely used manner for calculations of the pore size distribution in the mesoporous range.

lines 366-368:

on their surface or in their vicinity. An experimental investigation of the surface properties such as surface charge densities seems to be appropriate and valuable for investigating how surface properties (presence and types of functional groups) influence on the investigated chemical and physical phenomena.

lines 523-525:

performed according to the appropriate guidelines . Despite of the fact that the determination of surface area and pore size distribution is based on the physisorption measurements, the interpretation of the experimental isotherms is not always direct.

lines 658-660:

assumptions): (1) constant laminar flow, (2) absence of an external pressure, (3) negligible gravitational force and (4) the liquid at the solid-liquid interface does not move. The hydrostatic

pressure is much smaller than the capillary pressure, therefore, the capillary pressure causes that the liquid is rising upward along the tube. The wettability studies of small particles should always take in account the accuracy and reproducibility of results.

lines 691-693:

These results come from various structures of the pore wall. As follows from literature the melting temperature in the pores $T_{m,pore}$ is dependent on two variables: pore size H and wettability parameter α_w. For smaller α_w values ($\alpha_w << 1$) the depression of $T_{m,pore}$ is expected.

lines 710-714:

research such as glass transitions, the time-scale molecular motions, whose time length is at the order of tens of femtoseconds to nanoseconds, so that the experiments should be performed at frequencies in the range from MHz to THz. In such problems as the decomposition of the obtained spectra or the interpretation and quantitative analysis of the results, the technique resembles more common spectroscopies. However—the dielectric method investigates the collective fluctuations of molecules having a permanent dipole moment (polar liquids) and having long lifetime, that is a difference between common techniques.

3. Please address the additional comments in the attached manuscript.

We have answered on the all additional comments in the attached manuscript. The responses were implemented in the text (in the places particularly indicated).